Granger causality from the first and second derivatives of atmospheric CO_2 to global surface temperature, ENSO and NDVI

L.M.W. Leggett [1] and D.A. Ball [1]
(1) (Global Risk Policy Group Pty Ltd, Townsville, Queensland, Australia)
www.globalriskprogress.com
Correspondence to: L.M.W. Leggett (mleggett.globalriskprogress@gmail.com)

Abstract

A significant gap now of some 16 years in length has been shown to exist between the observed global surface temperature trend and that expected from the majority of climate simulations, and this gap is presently continuing to increase. For its own sake, and to enable better climate prediction for policy use, the reasons behind this mismatch need to be better understood. While an increasing number of possible causes have been proposed, the candidate causes have not yet converged.

The standard model which is now displaying the disparity has it that temperature will rise roughly linearly with atmospheric CO_2. However research also exists showing correlation between the interannual variability in the growth rate of atmospheric CO_2 and temperature. Rate of change of CO_2 had not been considered a causative mechanism for temperature because it was concluded that causality ran from temperature to rate of change of CO_2.

However more recent studies have found little or no evidence for temperature leading rate of change of CO_2 but instead evidence for simultaneity. With this background, this paper reinvestigated the relationship between rate of change of CO_2 and two of the major climate variables, atmospheric temperature and the El Niño–Southern Oscillation (ENSO).

Using time series analysis in the form of dynamic regression modelling with autocorrelation correction, it is demonstrated that first-derivative CO_2 leads temperature and that there is a highly statistically significant correlation between first-derivative CO_2 and temperature. Further, a correlation is found for second-derivative CO_2, with the Southern Oscillation Index, the atmospheric-pressure component of ENSO. This paper also demonstrates that both these correlations display Granger causality.

It is shown that the first-derivative CO_2 and temperature model shows no trend mismatch in recent years.

These results may contribute to the prediction of future trends for global temperature and ENSO.

Interannual variability in the growth rate of atmospheric CO_2 is standardly attributed to variability in the carbon sink capacity of the terrestrial biosphere. The terrestrial biosphere carbon sink is created by photosynthesis: a major way of measuring global terrestrial photosynthesis is by means of satellite measurements of vegetation reflectance, such as the Normalized Difference Vegetation Index (NDVI). This study finds Granger causality between an increasing NDVI and the increasing climate model/temperature difference (as quantified by the difference between the trend in the level of CO_2 and the trend in temperature).

It is believed that the results in this paper provide strong evidence that the global climate is the result of the combination of two mechanisms – one, a physical mechanism based on the level of atmospheric CO_2, the other a mechanism embodied in the terrestrial biosphere and based on the rate of change of CO_2

1 Introduction

Understanding current global climate requires an understanding of trends both in Earth's atmospheric temperature and the El Niño–Southern Oscillation (ENSO), a characteristic large-scale distribution of warm water in the tropical Pacific Ocean and the dominant global mode of year-to-year climate variability (Holbrook et al. 2009). However, despite much effort, the average projection of current climate models has become statistically significantly different from the 21st century global surface temperature trend (Fyfe et al., 2013, 2014) and has failed to reflect the statistically significant evidence that annual-mean global temperature has not risen in the 21st century (Fyfe 2013; Kosaka 2013).

The situation is illustrated visually in Figure 1 which shows the increasing departure over recent years of the global surface temperature trend from that projected by a representative climate model (the CMIP3, SRESA1B scenario model for global surface temperature (KNMI 2013)). It is noted that the level of atmospheric CO_2 is a good proxy for the IPCC models predicting the global surface temperature trend: according to IPCC AR5 (2014), on decadal to interdecadal time scales and under continually increasing effective radiative forcing, the forced component of the global surface temperature trend responds to the forcing trend relatively rapidly and almost linearly.

Modelling also provides a wide range of predictions for future ENSO variability, some showing an increase, others a decrease and some no change (Guilyardi et al 2012; Bellenger 2013). The extremes of this ENSO variability cause extreme weather (such as floods and droughts) in many regions of the world.

A wide range of physical explanations has now been proposed for the global warming slowdown. These involve proposals either for changes in the way the *radiative mechanism itself* is working or for the increased influence of *other physical mechanisms*. Chen and Tung (2014) place these proposed explanations into two categories. The first involves a reduction in radiative forcing: by a decrease in stratospheric water vapour, an increase in background stratospheric volcanic aerosols, by 17 small volcano eruptions since 1999, increasing coal-burning in China, the indirect effect of time-varying anthropogenic aerosols, a low solar minimum, or a combination of these. The second category of candidate explanation involves planetary sinks for the excess heat. The major focus for the source of this sink has been physical and has involved ocean heat sequestration. However, evidence for the precise nature of the ocean sinks is not yet converging: according to Chen and Tung

(2014) their study followed the original proposal of Meehl et al. (2011) that global deep-ocean heat sequestration is centred on the Pacific. However, their observational results were that such deep-ocean heat sequestration is mainly occurring in the Atlantic and the Southern oceans.

Alongside the foregoing possible physical causes, Hansen et al. (2013) have suggested that *the mechanism for* the pause in the global temperature increase since 1998 might be the planetary biota, in particular the terrestrial biosphere: that is (IPCC 2007), the fabric of soils, vegetation and other biological components, the processes that connect them and the carbon, water and energy they store.

It is widely considered that the interannual variability in the growth rate of atmospheric CO_2 is a sign of the operation of the influence of the planetary biota. Again, IPCC (2007) states: "The atmospheric CO_2 growth rate exhibits large interannual variations. The change in fossil fuel emissions and the estimated variability in net CO_2 uptake of the oceans are too small to account for this signal, which must be caused by year-to-year fluctuations in land-atmosphere fluxes."
In the IPCC Fourth Assessment Report, Denman *et al.* (2007) state (italics denote present author emphasis): "Interannual and inter-decadal variability in the growth rate of atmospheric CO_2 is dominated by the *response of the land biosphere to climate variations*. …. The terrestrial biosphere *interacts strongly with the climate*, providing both positive and negative feedbacks due to biogeophysical and biogeochemical processes. … Surface climate is determined by the balance of fluxes, which can be changed by radiative (e.g., albedo) or non-radiative (e.g., water cycle related processes) terms. Both radiative and non-radiative terms *are controlled by details of vegetation*."

Denman *et al.* (2007) also note that many studies have confirmed that the variability of CO_2 fluxes is mostly due to land fluxes, and that tropical lands contribute strongly to this signal. A predominantly terrestrial origin of the growth rate variability can be inferred from (1) atmospheric inversions assimilating time series of CO_2 concentrations from different stations (2) consistent relationships between δ13C and CO_2 (3) ocean model simulations and (4) terrestrial carbon cycle and coupled model simulations. For one prominent estimate carried out by the Global Carbon Project, the land sink is calculated as the residual of the sum of all sources minus the sum of the atmosphere and ocean sinks (Le Quere et al. 2014).

The activity of the land sink can also be estimated directly. The terrestrial biosphere carbon sink is created by photosynthesis: a major way of measuring global land photosynthesis is by means of satellite measurements of potential photosynthesis from greenness estimates. The predominantly used such measure is the Normalized Difference Vegetation Index (NDVI) (Running et al., 2004; Zhang et al. 2014). NDVI data are available from the start of satellite observations in 1980 to the present. For this period the trend signature in NDVI has been shown to correlate closely with that for atmospheric CO_2 (Barichivich et al., 2013). This noted, we have not been able to find studies which have compared NDVI data with the difference between climate models and temperature.

2 Methodological issues and objectives of the study

2.1 Methodological issues

Before considering further material it is helpful now to consider a range of methodological issues and concepts. The first concept is to do with the notion of causality.

According to Hidalgo and Sekhon (2011) there are four prerequisites to enable an assertion of causality. The first is that the cause must be prior to the effect. The second prerequisite is "constant conjunction" (Hume (1751) cited in Hidalgo and Sekhon (2011)) between variables. This relates to the degree of fit between variables. The final requirements are those concerning manipulation; and random placement into experimental and control categories. It is noted that each of the four prerequisites is necessary but not sufficient for causality.

Concerning the last two criteria, the problem for global studies such as global climate studies is that manipulation and random placement into experimental and control categories cannot be carried out.

One method using correlational data, however, approaches more closely the quality of information derived from random placement into experimental and control categories. The concept is that of Granger causality (Granger 1969). According to Stern and Kaufmann (2014) a time series variable "*x*" (e.g. atmospheric CO_2) is said to "Granger-cause" variable "*y*" (e.g. surface temperature) if past values of *x* help predict the current level of *y*, better than do just the past values of *y*, given all other relevant information.

Reference to the above four aspects of causality will be made to help structure the review of materials in the following sections.

2.2 Objectives of the study

What has been considered to influence the biota's creation of the pattern observed in the trend in the growth rate of atmospheric CO_2? The candidates for the influences on the biota have mainly been considered in prior research to be atmospheric variations, primarily temperature and/or ENSO (e.g., Kuo et al., 1990; Wang W. et al., 2013). Despite its proposed role in global warming overall, CO_2 (in terms of the initial state of atmospheric CO_2 exploited by plants at time *A*) has not generally been isolated and studied in detail through time series analysis as an influence in the way the biosphere influences the CO_2 left in the atmosphere at succeeding time *B*.

This state of affairs seems to have come about for two reasons, one concerning ENSO, the other, temperature. For ENSO, the reason is that the statistical studies are unambiguous that ENSO leads rate of change of CO_2 (e.g., Lean and Rind, 2008). On the face of it, therefore, this ruled out CO_2 as the first mover of the ecosystem processes. For temperature, the reason was that the question of whether atmospheric temperature leads rate of change of CO_2 or vice versa is less settled.

In the first published study on this question, Kuo et al. (1990) provided evidence that the signature of interannual atmospheric CO_2 (measured as its first derivative) fitted temperature (passing therefore one of the four tests for causality, of close conjunction).

The relative fits of both level of and first derivative of atmospheric CO_2 with global surface temperature up to the present are depicted in Figure 2. Attention is drawn to both signature (fine grained data structure) and, by means of polynomial smoothing, core trend for each data series.

Concerning signature, while clearly first-derivative CO_2 and temperature are not identical, each is more alike than either is to the temperature model based on level of CO_2. As well, the polynomial fits show that the same likeness groupings exist for core trend.

Kuo et al. (1990) also provided evidence concerning another of the causality prerequisites – priority. This was that the signature of first-derivative CO_2 *lagged* temperature (by 5 months). This idea has been influential. More recently, despite Adams and Piovesan (2005) noting that climate variations, acting on ecosystems, are believed to be responsible for variation in CO_2 increment, but there are major uncertainties in identifying processes including uncertainty concerning *instantaneous* (present authors' emphasis) versus lagged responses; and Wang W. et al (2013) observing that the strongest coupling is found between the CO_2 growth rate and the *concurrent* (present authors' emphasis) tropical land temperature, Wang et al 2013 nonetheless state in their conclusion that the strong temperature–CO_2 coupling they observed is best explained by the additive responses of tropical terrestrial respiration and primary production to temperature variations, which reinforce each other in enhancing *temperature's control* (present author emphasis) on tropical net ecosystem exchange.

Another perspective on the relative effects of rising atmospheric CO_2 concentrations on the one hand and temperature on the other has been provided by extensive direct experimentation on plants. In a large scale meta-analysis of such experiments, Dieleman et al. (2012) drew together results on how ecosystem productivity and soil processes responded to combined warming and CO_2 manipulation, and compared it with those obtained from single factor CO_2 and temperature manipulation. While the meta-analysis found that responses to combined CO_2 and temperature treatment showed the greatest effect, this was only slightly larger than for the CO_2-only treatment. By contrast the effect of the CO_2-only treatment was markedly larger than for the warming-only treatment.

Concerning leading and lagging climate series more generally, the first finding of correlations between the rate of change (in the form of the first derivative) of atmospheric CO_2 and a climate variable was with the foregoing and the Southern Oscillation Index (SOI) component of ENSO (Bacastow 1976). Here evidence was presented that the SOI led first-derivative atmospheric CO_2. There have been further such studies (see Imbers (2013) for overview) which, taken together, consistently show that the highest correlations are achieved with SOI leading temperature, by some months (3-4 months).

In light of the foregoing this paper reanalyses by means of time series regression analysis the question of which of first-derivative CO_2 and temperature leads which, The joint temporal relationship between interannual atmospheric CO_2, global surface temperature and ENSO (indicated by the SOI) is also investigated.

The foregoing also shows that a strong case can be made for further investigating the planetary biota influenced by atmospheric CO_2 as a candidate influence on (cause of) climate outcomes. This question is also explored in this paper.
A number of Granger causality studies have been carried out on climate time series (see review in Attanasio 2012). Of papers we have found which assessed atmospheric CO_2 and global surface temperature – some six (Sun and Wang 1996; Triacca 2005; Kodra et al., 2011; Attanasio and Triacca, 2011; Attanasio (2012); Stern and Kaufmann 2014) –while all but one (Triacca 2005) found Granger causality, it was not with CO_2 concentration but with CO_2 radiative forcing ($\ln CO_2$ (Attanasio and Triacca, 2011).

As well, all studies used annual not monthly data. Such annual data for each of atmospheric CO_2 and temperature is not stationary of itself but must be made stationary by differencing (Sun and Wang 1996). Further, data at this level of aggregation can "mask" correlational effects that only become apparent when higher frequency (e.g., monthly) data are used.

Rather than using a formal Granger causality analysis, a number of authors have instead used conventional multiple regression models in attempts to quantify the relative importance of natural and anthropogenic influencing factors on climate outcomes such as global surface temperature. These regression models use contemporaneous explanatory variables. For example, see Lean and Rind (2008, 2009); Foster and Rahmstorf (2011); Kopp and Lean (2011); Zhou and Tung (2013). This type of analysis effectively assumes a causal direction between the variables being modelled. It is incapable of providing a proper basis for testing for the presence or absence of causality. In some cases account has been taken of autocorrelation in the model's errors, but this does not overcome the fundamental weakness of standard multiple regression in this context. In contrast, Granger causality analysis that we adopt in this paper provides a formal testing of both the presence and direction of this causality (Granger, 1969).

Short of Granger causality analysis, another method of assessment used has been multiple linear regression, either corrected or uncorrected for autocorrelation. This method has frequently been used to quantify the relative importance of natural and anthropogenic influencing factors on climate outcomes such as global surface temperature – for example, Lean and Rind, (2008), Lean and Rind (2009); Foster and Rahmstorf, (2011); Kopp and Lean, (2011); Zhou and Tung (2013)). It is noted that while multiple regression analysis can at best *assume* a causal direction between the variables being modelled, Granger causality analysis provides a formal testing of this assumption (Granger 1969).

From such studies, a common set of main influencing factors (also called explanatory or predictor variables) has emerged. These are (Lockwood (2008); Folland (2013); Zhou and Tung (2013): El Nino–Southern Oscillation (ENSO), or Southern Oscillation alone (SOI); volcano aerosol optical depth; total solar irradiance; and the trend in anthropogenic greenhouse gas (the predominant anthropogenic greenhouse gas being CO_2). In these models, ENSO/SOI is the factor embodying interannual variation. Imbers et al. (2013) show that a range of different studies using these variables have all produced similar and close fits with the global surface temperature.

With this background this paper first presents an analysis concerning whether the first derivative of atmospheric CO_2 leads or lags global surface temperature. That assessed, questions of autocorrelation, strength of correlation, and of causality are then explored.

Given this exploration of correlations involving first-derivative atmospheric CO_2, the possibility of the correlation of second difference CO_2 with climate variables is also explored.

Correlations are assessed at a range of time scales to seek the time extent over which relationships are held, and thus whether they are a special case or possibly longer term in nature. The time scales involved are, using instrumental data, over two periods starting respectively from 1959 and 1877; and, using paleoclimate data, over a period commencing from 1515. The correlations are assessed by means of regression models explicitly incorporating autocorrelation using dynamic modelling methods. Granger causality between CO_2 and, respectively, temperature and SOI is also explored. Atmospheric CO_2 rather than emissions data is used, and where possible at monthly rather than annual aggregation. Finally, as noted, we have not been able to find studies which have compared the gap between climate models and temperature with NDVI data so an assessment of this question is carried out. All assessments were carried out using the time series statistical software packages Gnu Regression, Econometrics and Time-series Library (GRETL) and IHS Eviews.

3. Data and methods

We present results of time series analyses of climate data. The data assessed are global surface temperature, atmospheric carbon dioxide (CO_2) and the Southern Oscillation Index (SOI). The regressions are presented in several batches based on the length of data series for which the highest temporal resolution is available. The first batch of studies involves the data series for which the available high resolution series is shortest: this is for atmospheric carbon dioxide (CO_2) and commences in 1958. These studies are set at monthly resolution.

The second batch of studies is for data able to be set at monthly resolution not involving CO_2. These studies begin with the time point at which the earliest available monthly SOI data commences, 1877.

The final batch of analyses utilises annual data. These studies use data starting variously in the 16th or 18th centuries.

Data from 1877 and more recently is from instrumental sources; earlier data is from paleoclimate sources.

For instrumental data sources for global surface temperature we used the Hadley Centre–Climate Research Unit combined land SAT and SST (HadCRUT) version 4.2.0.0 (Morice et al., 2012), for atmospheric CO_2 the U.S. Department of Commerce National Oceanic & Atmospheric Administration Earth System Research Laboratory Global Monitoring Division Mauna Loa, Hawaii monthly CO_2 series (Keeling et al., 2009), and for volcanic aerosols the National Aeronautic and Space Administration Goddard Institute for Space Studies Stratospheric Aerosol Optical Thickness series (Sato et al., 1993). Southern Oscillation Index (SOI) data (Troup 1965) is from the Science Delivery Division of the Department of Science, Information Technology, Innovation and the Arts (DSITIA) Queensland Australia. Solar irradiance data is from Lean, J. (personal communication 2012).

The Southern Oscillation is the atmospheric-pressure component of ENSO, and is an oscillation in the surface air pressure between the tropical eastern and the western Pacific Ocean waters. It is calculated from normalized Tahiti minus Darwin sea level pressure. The SOI only takes into account sea-level pressure. In contrast, the El Niño component of ENSO is specified in terms of changes in the Pacific Ocean sea surface temperature relative to the average temperature. It is considered to be simpler to conduct an analysis in which the temperature is an outcome (dependent variable) without also having (Pacific Ocean) temperature as an input (independent variable). The correlation between SOI and the other ENSO indices is high, so we believe this assumption is robust.

Paleoclimate data sources are: Atmospheric CO_2, from 1500: ice cores (Robertson et al. (2001).; (NH) temperature, from 1527: tree ring data: Moberg, A., et al. 2005; SOI, from 1706: tree ring data: Stahle et al. (1998).

Normalized Difference Vegetation Index (NDVI) monthly data from 1980 to 2006 is from the GIMMS (Global Inventory Modeling and Mapping Studies) data set, accessed via KNMI (2014). NDVI data from 2006 to 2013 was provided by the Institute of Surveying, Remote Sensing and Land Information, University of Natural Resources and Life Sciences, Vienna.

Statistical methods used are standard (Greene 2012). Categories of methods used are: normalisation; differentiation (approximated by differencing); and time series analysis. Within time series analysis, methods used are: smoothing; leading or lagging of data series relative to one another to achieve best fit; assessing a prerequisite for using data series in time series analysis, that of stationarity; including autocorrelation in models by use of dynamic regression models; and investigating causality by means of a multivariate time series model, known as a vector autoregression (VAR) and its associated Granger causality test. These methods will now be described in turn.

To make it easier to visually assess the relationship between the key climate variables, the data were normalised using statistical Z scores or standardised deviation scores (expressed as "Relative level" in the figures). In a Z-scored data series, each data point is part of an overall data series that sums to a zero mean and variance of 1, enabling comparison of data having different native units. Hence, when several Z-scored time series are depicted in a graph, all the time series will closely superimpose, enabling visual inspection to clearly discern the degree of similarity or dissimilarity between them.

See the individual figure legends for details on the series lengths.

In the time series analysis SOI and global atmospheric surface temperature are the dependent variables. For these two variables, we tested the relationship between (1) the change in atmospheric CO_2 and (2) the variability in its rate of change. We express these CO_2-related variables as finite differences, which is a convenient approximation to derivatives (Hazewinkel, 2001; Kaufmann et al., 2006). The finite differences used here are of both the first- and second-order types (we label these "first" and "second" differences in the text). Variability is explored using both intra-annual (monthly) data and interannual (yearly) data. The period covered in the figures is shorter than that used in the data preparation because of the loss of some data points due to calculations of differences and of moving averages (in monthly terms of up to 13 x 13), which commenced in January 1960.

Smoothing methods are used to the degree needed to produce similar amounts of smoothing for each data series in any given comparison. Notably, to achieve this outcome, series resulting from higher levels of differences require more smoothing. Smoothing is carried out initially by means of a 13-month moving average – this also minimises any remaining seasonal effects. If further smoothing is required, then this is achieved (Hyndman 2010) by taking a second moving average of the initial moving average (to produce a double moving average). Often, this is performed by means of a further 13 month moving average to produce a 13 x 13 moving average. For descriptive statistics to describe the long-term variation of a time series trend, polynomial smoothing is sometimes used.

It is important to consider what effects this filtering of our data may have on the ensuing statistical analysis. In these analyses, only the CO_2 series was smoothed and therefore requires assessment. To do this we tested if the smoothed (2 x 13 month moving average) first-derivative CO_2 series used here has different key dynamics to that of the original raw (unsmoothed) data from which the smoothed series was derived. Lagged correlogram analysis showed that the maximum, and statistically significant, correlation of the smoothed series with the unsmoothed series occurs when there is no phase shift. This suggests that the particular smoothing used should provide no problems in the assessment of which of first difference CO_2 and temperature has priority.

Second, there is extensive evidence that while the effect that seasonal adjustment (via smoothing) on the usual tests for unit roots in time-series data is to reduce their power in small samples, this distortion is *not* an issue with samples of the size used in this study. For example, see Ghysels (1990), Frances (1991), Ghysels and Perron (1993), and Diebold (1993). Moreover, Olekalns (1994) shows that seasonal adjustment by using dummy variables also impacts adversely on the finite-sample power of these tests, so there is little to be gained by considering this alternative approach. Finally, one of the results emerging from the Granger causality literature is that while such causality can be "masked" by the smoothing of the data, apparent causality cannot be "created" from non-causal data. For example, see Sims (1971), Wei (1982), Christiano and Eichenbaum (1987), Marcellino (1999), Breitung and Swanson (2002), and Gulasekaran and Abeysinghe (2002). This means that our results relating to the existence of Granger causality should not be affected adversely by the smoothing of the data that has been undertaken.

Variables are led or lagged relative to one another to achieve best fit. These leads or lags were determined by means of time-lagged correlations (correlograms). The correlograms were calculated by shifting the series back and forth relative to each other, 1 month at a time.

With this background, the convention used in this paper for unambiguously labelling data series and their treatment after smoothing or leading or lagging is depicted in the following example. The atmospheric CO_2 series is transformed into its second derivative and smoothed twice with a 13 month moving average. The resultant series is then Z-scored. This is expressed as Z2x13mma2ndDerivCO_2.

As well, it is noted that, to assist readability in text involving repeated references, atmospheric CO_2 is sometimes referred to simply as CO_2 and global surface temperature as temperature.

The time series methodology used in this paper involves the following procedures. First, any two or more time series being assessed by time series regression analysis must be what is termed stationary in the first instance, or be capable of being made stationary (by differencing). A series is stationary if its properties (mean, variance, covariances) do not change with time (Greene 2012). The (augmented) Dickey-Fuller test is applied to each variable. For this test, the null hypothesis is that the series has a unit root, and hence is non-stationary. The alternative hypothesis is that the series is integrated of order zero.

Second, the residuals from any time series regression analysis then conducted must not be significantly different from white noise. This is done seeking correct model specification for the analysis.

After Greene (2012): the results of standard ordinary least squares (OLS) regression analysis assume that the errors in the model are uncorrelated. Autocorrelation of the errors violates this assumption. This means that the OLS estimators are no longer the Best Linear Unbiased Estimators (BLUE). Notably and importantly this does not bias the OLS coefficient estimates. However statistical significance can be overestimated, and possibly greatly so, when the autocorrelations of the errors at low lags are positive.

Addressing autocorrelation can take either of two alternative forms: *correcting for it* (for example, for first order autocorrelation by the Cochrane-Orcutt procedure), or *taking it into account*.

In the latter approach, the autocorrelation is taken to be a consequence of an inadequate specification of the temporal dynamics of the relationship being estimated. The method of dynamic modelling (Pankratz, 1991) addresses this by seeking to explain the current behavior of the dependent variable in terms of both contemporaneous and past values of variables. In this paper the dynamic modelling approach is taken.

To assess the extent of autocorrelation in the residuals of the initial non-dynamic OLS models run, the Breusch-Godfrey procedure is used. Dynamic models are then used to take account of such autocorrelation. To assess the extent to which the dynamic models achieve this, Kiviet's Lagrange multiplier F-test (LMF) statistic for autocorrelation (Kiviet, 1986) is used.

Hypotheses related to Granger causality (see Introduction) are tested by estimating a multivariate time series model, known as a vector autoregression (VAR), for level of, and first-derivative CO_2 and other relevant variables. The VAR models the current values of each variable as a linear function of their own past values and those of the other variables. Then we test the hypothesis that x does not cause y by evaluating restrictions that exclude the past values of x from the equation for y and vice versa.

Stern and Kander (2011) observe that Granger causality is not identical to causation in the classical philosophical sense, but it does demonstrate the likelihood of such causation or the lack of such causation more forcefully than does simple contemporaneous correlation. However, where a third variable, *z*, drives both *x* and *y*, *x* might still appear to drive *y* though there is no actual causal mechanism directly linking the variables (any such third variable must have some plausibility - see Discussion and conclusions below).

4 Results

4.1. Relationship between first-derivative CO_2 and temperature

4.1.1. Priority

Figure 2 showed that while clearly first-derivative CO_2 and temperature are not identical in signature, each is more alike than either is to the temperature model based on level of CO_2. As well the figure shows that the same likeness relationships exist for the core trend. The purpose of the forthcoming sections is to see the extent to which these impressions are statistically significant.

The first question assessed is that of priority: which of first-derivative atmospheric CO_2 and global surface temperature leads the other. The two series are shown for the period 1959 to 2012 in Figure 3.

It is not possible to discern from the above plot which precise relative phasing of the two series leads to the best fit and hence the answer to the question of which series leads which. To quantify the degree of difference in phasing between the variables, time-lagged correlations (correlograms) were calculated by shifting the series back and forth relative to each other, one month at a time.

First, what does the above relationship look like in correlogram form, and what is the appearance of the correlograms for the other commonly used global temperature categories – tropical, Northern hemisphere and Southern hemisphere? These correlograms are given in Figure 4.

It can be seen that, for all four relationships shown, first-derivative CO_2 always leads temperature. The leads differ as quantified in Table 1.

It is possible for a lead to exist overall on average but for a lag to occur for one or other specific subsets of the data. This question is explored in Figure 5 and Table 2. Here the full 1959-2012 period of monthly data– some 640 months – for each of the temperature categories is divided into three approximately equal sub-periods, to provide 12 correlograms. It can be seen that in all 12 cases, first-derivative CO_2 leads temperature. It is also noted that earlier sub-periods tend to display longer first-derivative CO_2 leads. For the most recent sub-period the highest correlation is when the series are neither led nor lagged.

4.1.2 Correspondence between first-derivative CO_2 and global surface temperature curves

Next, the second prerequisite for causality, close correspondence, is also seen between first-derivative CO_2 and global surface temperature in Figure 3.

4.1.3 Time series analysis

The robustness of both first-derivative CO_2 leading temperature and the two series displaying close correspondence is a firm basis for the time series analysis to follow of the statistical relationship between first-derivative CO_2 and temperature. For this further analysis we choose global surface temperature as the temperature series because, while its maximum correlation is not the highest (Figure 5), its global coverage by definition is greatest.

The following sections provide the results of the time series analysis. (In this section, TEMP stands for global surface temperature ((Hadcrut4), and other block capital terms are those used in the modelling.) First, as stated above, all series used in a time series regression must be stationary (Greene 2012). By means of the Augmented Dickey–Fuller (ADF) test for unit roots Table 3 provides the information concerning the stationarity for the level of, and first-derivative of, CO_2, as well as global surface temperature. The test was applied with an allowance for both a drift and deterministic trend in the data, and the degree of augmentation in the Dickey-Fuller regressions was determined by minimizing the Schwarz Information Criterion.

The table shows that, for the monthly series used, the variables TEMP and FIRSTDERIVATIVE CO_2 are both stationary.
In carrying this out, one must first note that while we find, as is required for time series analysis, that the variables TEMP and FIRSTDERIVATIVE CO_2 are both stationary, (that is, both display order of integration of *I (1)*), Beenstock et al. (2012) report in their work that temperature *is I(1)* while first-difference (equivalent to first-derivative) atmospheric CO_2 is *I*(2).

With regard to the reconciliation of these two varying results, Pretis and Hendry (2013) have reviewed Beenstock et al. (2012). They take issue with the finding of *I(2)*, and find evidence that it results from the combination of two different data sets measured in different ways to make up the tested 1850-2011 data set which Beenstock et al. use. Regarding this composite series they write:

> In the presence of these different measurements exhibiting structural changes, a unit-root test on the entire sample could easily not reject the null hypothesis of *I*(2) even when the data are in fact *I(1)*. Indeed, once we control for these changes, our results contradict the findings in Beenstock et al. (2012).

In contrast, the variable CO_2 is non-stationary (specifically, it is integrated of order one, i.e., I(1)). Here an important result arises: attempting to assess TEMP in terms of the level of CO_2 would result in an "unbalanced regression", as the dependent variable (TEMP) and the explanatory variable (CO_2) have different orders of integration. It is well known (e.g., Banerjee et al., 1993, pp. 190-191, and the references therein) that in unbalanced regressions the t-statistics are biased away from zero. That is, one can appear to find statistically significant results when in fact they are not present. In fact, that occurs when we regress TEMP on CO_2. This reason alone is strong evidence that any analysis should involve the variables TEMP and FIRST-DERIVATIVE CO_2, and not TEMP and CO_2.

Nonetheless one can explore the extent to which first-derivative CO_2 and climate variable correlations are statistically significant and so might make first-derivative CO_2 a candidate in its own right as a cause of climate trends.

For the variables for which stationarity is established, one must next assess the extent if any of autocorrelation affecting the time series model. This is done by obtaining diagnostic statistics from an OLS regression. This regression shows, by means of the Breusch-Godfrey test for autocorrelation (up to order 12 - that is, including all monthly lags up to 12 months), that there is statistically significant autocorrelation at lags of one and two months, leading to an overall Breusch-Godfrey Test statistic (LMF) = 126.901238, with p-value = P(F(12,626) > 126.901) = 1.06e-158.

The autocorrelation is taken to be a consequence of an inadequate specification of the temporal dynamics of the relationship being estimated. With this in mind, a dynamic model (Greene 2012) with two lagged values of the dependent variable as additional independent variables has been estimated.

Results are shown in Table 4. There, the LMF test shows that there is now no statistically significant unaccounted-for autocorrelation, thus supporting the use of this dynamic model specification.

Inspection of Table 4 shows that a highly statistically significant model has been established. First it shows that the temperature in a given period is strongly influenced by the temperature of closely preceding periods. (See Discussion for a possible mechanism for this). Further it provides evidence that there is also a clear, highly statistically significant role in the model for first-derivative CO_2.

4.1.4 Granger causality analysis

We now can turn to assessing if first-derivative atmospheric CO_2 may not only correlate with, but also contribute causatively to, global surface temperature. This is done by means of Granger causality analysis.

Recalling that both TEMP and FIRST-DERIVATIVE CO_2 are stationary, it is appropriate to test the null hypothesis of no Granger causality from FIRST-DERIVATIVE CO_2 to TEMP by using a standard Vector Autoregressive (VAR) model without any transformations to the data. The Akaike information criterion (AIC) and the Schwartz information criterion (SIC) were used to select an optimal maximum lag length (k) for the variables in the VAR. This lag length was then lengthened, if necessary, to ensure that:

(i) The estimated model was dynamically stable (i.e., all of the inverted roots of the characteristic equation lie inside the unit circle);
(ii) The errors of the equations were serially independent.

The relevant EViews output from the VAR model is entitled VAR Granger Causality/Block Exogeneity Wald Tests and documents the following summary results: Wald Statistic (p-value): Null is there is No Granger Causality from first-derivative CO_2 to TEMP Number of lags K=4; Chi-Square 26.684 (p-value = 0.000).

A p-value of this level is highly statistically significant and means the null hypothesis of No Granger Causality is very strongly rejected. That is, over the period studied there is strong evidence that first-derivative CO_2 Granger-causes TEMP.

Despite the lack of stationarity in the level of CO_2 time series meaning it cannot be used to model temperature, one can still assess the answer to the question: “Is there evidence of Granger causality between level of CO_2 and TEMP?”

In answering this question, because the TEMP series is stationary, but the CO_2 series is non-stationary (it is integrated of order one, I(1)), the testing procedure is modified slightly. Once again, the levels of both series are used. For each VAR model, the maximum lag length (k) is determined, but then one additional lagged value of both TEMP and CO_2 is included in each equation of the VAR. However, the Wald test for Granger non-causality is applied only to the coefficients of the original k lags of CO_2. Toda and Yamamoto (1995) show that this modified Wald test statistic will still have an asymptotic distribution that is chi-square, even though the level of CO_2 is non-stationary.

Here the relevant Wald Statistic (p-value): Null is there is No Granger Causality from level of CO_2 to TEMP Number of lags K= 4; Chi-Square 2.531 (p-value = 0.470)

The lack of statistical significance in the p-value is strong evidence that level of CO_2 does not Granger-cause TEMP.

With the above two assessments done, it is significant that concerning global surface temperature we are able to discount causality involving the level of CO_2, but establish causality involving first-derivative CO_2.

4.2 Relationship between second-derivative CO_2 and temperature and Southern Oscillation Index

4.2.1 Priority and correspondence

Given the results of this exploration of correlations involving first-derivative atmospheric CO_2, the possibility of the correlation of second-derivative CO_2 with climate variables is also explored. The climate variables assessed are global surface temperature and the Southern Oscillation Index (SOI). In this section, data is from the full period for which monthly instrumental CO_2 data is available, 1958 to the present. For this period, the series neither led nor lagged appear as follows (Figure 6):

Let us look (Figure 6) at the two key pairs of interannually varying factors. For the purpose of this figure, to facilitate depiction of trajectory, second-derivative CO_2 and SOI (right axis) are offset so that all four curves display a similar origin in 1960.

The figure shows that, alongside the already demonstrated close similarity between first-derivative CO_2 and temperature, there is a second apparent distinctive pairing between second-derivative CO_2 and SOI.

The figure shows that the overall trend, amplitude and phase - the signature - of each pair of curves is both matched within each pair and different from the other pair. The remarkable sorting of the four curves into two groups is readily apparent. Each pair of results provides context for the other - and highlights the different nature of the other pair of results.

Recalling that even uncorrected for any autocorrelation, correlational data still holds information concerning regression coefficients, we initially use OLS correlations without assessing autocorrelation to provide descriptive statistics. Table 5 includes, first without any phase shifting to seek to maximise fit, the full six pairwise correlations arising from all possible combinations of the four variables other than with themselves. Here it can be seen that the two highest correlation coefficients (in bold in the table) are, first, between first-derivative CO_2 and temperature, and, second, between second-derivative CO_2 and SOI.

In Table 6 phase shifting has been carried out to maximise fit (shifts shown in variable titles in the table). This results in an even higher correlation coefficient for second-derivative CO_2 and SOI.

The link between all three variable realms — CO_2, SOI and temperature — can be further observed in Figure 7 and Table 7. Figure 7 shows SOI, second-derivative atmospheric CO_2 and first-derivative temperature, each of the latter two series phase-shifted for maximum correlation with SOI (as in Table 5). Concerning priority, Table 6 shows that maximum correlation occurs when second-difference CO2 leads SOI. It is also noted that the correlation coefficients for the correlations between the curves shown in Table 6 have all converged in value compared to those shown in Table 5.

Concerning differences between the curves shown in Figure 7, two of what major departures there are between the curves are coincide with volcanic aerosols – from the El Chichon volcanic eruption in 1982 and the Pinatubo eruption in 1992 (Lean and Rind 2009). These factors taken into account, it is notable when expressed in the form of the transformations in Figure 7 that the signatures of all three curves are so essentially similar that it is almost as if all three curves are different versions of - or responses to - the same initial signal.

So, a case can be made that first and second-derivative CO_2 and temperature and SOI respectively are all different aspects of the same process.

4.2.2 Time series analysis

Let us more formally assess the relationship between second-derivative CO_2 and SOI. As for first-derivative CO_2 and temperature above, stationarity has been established. Again, similarly to first-derivative CO_2 and temperature, there is statistically significant autocorrelation at lags of one and two months, leading to an overall Breusch-Godfrey Test statistic (LMF) of 126.9, with p-value = P(F(12,626) > 126.901) = 1.06e-158.

Table 8 shows the results of a dynamic model with the dependent variable used at each of the two lags as further independent variables.

In Table 8 the results first show (LMF test) that there is now no statistically significant unaccounted-for autocorrelation.

Further inspection of Table 8 shows that a highly statistically significant model has been established. As for temperature, it shows that the SOI in a given period is strongly influenced by the SOI of closely preceding periods. Again as for temperature it provides evidence that there is a clear role in the model for second-derivative CO_2.

With this established, it is noted that while the length of series in the foregoing analysis was limited by the start date of the atmospheric CO_2 series (January 1958), high temporal resolution (monthly) SOI goes back considerably further, to 1877. This long period SOI series (for background see Troup (1965)) is that provided by the Australian Bureau of Meteorology, sourced here from the Science Delivery Division of the Department of Science, Information Technology, Innovation and the Arts, Queensland, Australia. As equivalent temperature data is also available (the global surface temperature series already used above (HADCRUT4) goes back as far as 1850), these two longer series are now plotted in Figure 8.

What is immediately noted is the continuation over this longer period of the striking similarity between the two signatures already shown in Figure 7.

Turning to regression analysis, as previously the Breusch-Godfrey procedure shows that, for lags up to lag 12, the lion's share of autocorrelation is again restricted to the first two lags. Table 9 shows the results of a dynamic model with the dependent variable used at each of the two lags as further independent variables

In comparison with Table 8, the extended time series modelled in Table 9 shows a remarkably similar R-squared statistic: 0.466 compared with 0.477. By contrast, the partial regression coefficient for second-derivative CO_2 has increased, to 0.14 compared with 0.077. These points made, the main finding is that there is little or no difference in the relationship when it is extended back to 1877. (It is beyond the scope of this study, but the relationship of SOI and second-derivative CO_2 means it is now possible to produce a proxy for monthly atmospheric CO_2 from 1877: a date approximately 75 years prior to the start in January 1958 of the CO_2 monthly instrumental record.)

4.2.3 Granger causality analysis

This section assesses whether second-derivative CO_2 can be considered to Granger-cause SOI. This assessment is carried out using 1959 to 2012 data.

Test results on the stationarity or otherwise of each series are given in Table 10. Each series is shown to be stationary. These results imply that we can approach the issue of possible Granger causality by using a conventional VAR model, in the levels of the data, with no need to use a "modified" Wald test (as used in the Toda and Yamamoto (1995) methodology).

Simple OLS regressions of SOI against separate lagged values of DCO2 (including an intercept) confirm the finding that the highest correlation is when a two-period lag is used.

A 2-equation VAR model is needed for reverse-sign SOI and second-derivative CO_2. The first task is to determine the optimal maximum lag length to be used for the variables. Using the SIC, this is found to be 2 lags. When the VAR model is estimated with this lag structure however, Table 11, testing the null hypothesis that there is no serial correlation at lag order h, shows that there is evidence of autocorrelation in the residuals.

This suggests that the maximum lag length for the variables needs to be increased. The best results (in terms of lack of autocorrelation) were found when the maximum lag length is 3. (Beyond this value, the autocorrelation results deteriorated substantially, but the conclusions below, regarding Granger causality, were not altered.)

Table 12 shows that the preferred, 3-lag model, still suffers a little from autocorrelation.

However, as we have a relatively large sample size, this will not impact adversely on the Wald test for Granger causality.

The relevant EViews output from the VAR model is entitled VAR Granger Causality/Block Exogeneity Wald Tests and documents the following summary results: Wald Statistic (p-value): Null is there is No Granger Causality from second-derivative CO_2 to sign-reversed SOI Chi-Square 22.554 (p-value = 0.0001).

The forgoing Wald statistic shows that the null hypothesis is strongly rejected: in other words, there is very strong evidence of Granger Causality from second-derivative CO_2 to sign-reversed SOI.

4.3 Paleoclimate data

So far, the time period considered in this study has been pushed back in the instrumental data realm to 1877. If non-instrumental paleoclimate proxy sources are used, CO_2 data now at annual frequency can be taken further back. The following example uses CO_2 and temperature data. The temperature reconstruction used here commences in 1500 and is that of Frisia et al. (2003), derived from annually laminated speliothem (stalagmite) records. A second temperature record (Moberg et al., 2005) is from tree ring data. The atmospheric CO_2 record (Robertson et al. (2001) is from fossil air trapped in ice cores and from instrumental measurements. The trends for these series are shown in Figure 9.

Visual inspection of the figure shows that there is a strong overall likeness in signature between the two temperature series, and between them and first-derivative CO_2. The similarity of signature is notably less with level of CO_2. It can be shown that level of CO_2 is not stationary and even with the two other series which are stationary the strongly smoothed nature of the temperature data makes removal of the autocorrelation present impossible. Nonetheless, noting that data uncorrected for autocorrelation still provides valid correlations (Greene 2012) – only the statistical significance is uncertain - it is simply noted that first-derivative CO_2 displays a better correlation with temperature than level of CO_2 , for each temperature series (Table 13).

4.4 Normalized Difference Vegetation Index (NDVI)

Using the Normalized Difference Vegetation Index (NDVI) time series as a measure of the activity of the land biosphere, this section now investigates the land biosphere as a candidate mechanism for the issue identified in the Introduction, that of the increasing difference between the global surface temperature trend suggested by general circulation climate models and that observed.

The level of atmospheric CO_2 is a good proxy for the IPCC models predicting the global surface temperature trend: according to IPCC (2013), on decadal to interdecadal time scales and under continually increasing effective radiative forcing

(ERF), the forced component of the global surface temperature trend responds to the ERF trend relatively rapidly and almost linearly. This trend can be taken to represent that expected from the operation of the standard anthropogenic global warming model, its mechanism being a physical one in which (IPCC, 2013, NASA 2015) about half the light reaching Earth's atmosphere passes through the air and clouds to the surface, where it is absorbed and then radiated upward in the form of infrared heat. About 90 percent of this heat is then absorbed by the greenhouse gases and radiated back toward the surface, which is warmed. If greenhouse gases have been increasing (including because of increasing anthropogenic emissions), that contributes to an increase in the infrared radiation they emit (including that back toward the surface, which is warmed further).On this basis an indicator of the difference between the climate model trend and the observed temperature is prepared by subtracting the Z-scored actual temperature trend from the Z-scored CO_2 trend. In the paper, this indicator is sometimes termed the climate model/temperature difference or the difference between the level-of-CO_2 model for temperature and the observed temperature

The trend in the terrestrial CO_2 sink is estimated annually as part of assessment of the well known global carbon budget (Le Quere at al., 2014). It is noted that there is a risk of involving a circular argument concerning correlations between the terrestrial CO_2 sink and interannual (first derivative) CO_2 because the terrestrial CO_2 sink is defined as the residual of the global carbon budget (Le Quere at al., 2014). By contrast, the Normalized Difference Vegetation Index (NDVI) involves direct (satellite-derived) measurement of terrestrial plant activity. For this reason, and because of the two series only NDVI is provided in monthly form, we will use only NDVI in what follows.

4.4.1. Issues of method concerning the NDVI-related analyses

Two issues of method arise from the NDVI-related analyses. These are: sensitivity of methods for detecting the order of integration of a time series; and, for the Granger

Causality testing used, the optimal selection of the number of lags of the time series variables involved for use in the analysis.

These two matters will be dealt with in turn.

4.4.1.1. Determination of order of integration of time series.

The data series used until now – the shortest monthly series starting in 1959 – have meant that, using the most commonly used test of series order of integration (the Augmented Dickey-Fuller test (Dickey and Fuller, 1981)) it has been unambiguous as to the order of integration of each series.

The more recent start date arising from the use of the NDVI series – 1981 – has meant that the series used in the NDVI-related analyses have been made up of fewer observations, and are centred over a different period of history compared with the data commencing in 1959.

This has meant that one series – first-derivative CO_2 – for the data commencing in 1981 has displayed ADF unit root test results which place it on the cusp between I(0) and I(1).

According to Zivot and Wang (2006), the ADF test and another test, the Phillips-Perron test (Phillips and Perron (1988)) have in general very low power to discriminate between I(0) and I(1) alternatives when the two alternatives are close together. Zivot and Wang (2006) recommend that for maximum power in these circumstances the tests of Elliot, Rothenberg, and Stock (1996), and Ng and Perron (2001) should be used.

For this reason, the above - and some further - unit root tests for the order of integration of a time-series are used in this stage of the study. The full list of tests is:

- the Augmented Dickey Fuller (ADF) test (Dickey and Fuller ,1981); the Phillips-Perron test (Phillips and Perron, 1988); the Elliott-Rothenberg-Stock

Point Optimal test (Elliot et al., 1996); the Ng-Perron Modified Unit Root test (Ng and Perron, 2001). The null hypothesis for the foregoing tests is non-stationarity.

- The Kwiatkowski–Phillips–Schmidt–Shin (KPSS) test (Kwiatkowski et al., 1992) is also used. The null hypothesis for this test is stationarity.

Use of both stationarity and non-stationarity hypotheses can add robustness to the assessment of the order of integration of a time-series.

For the KPSS and Phillips-Perron tests the bandwidth, b, was selected using the Newey-West method, with the Bartlett kernel. In the remaining unit root tests the Akaike information criterion (AIC) and the Schwartz information criterion (SIC) were used to select an optimal maximum lag length (k) for the variables.

4.4.1.2. Lag-length selection for Granger causality testing

We turn now to a matter concerning lag-length selection for Granger causality testing.

Thornton and Batten (1985) assessed the accuracy of Granger tests under a range of lag selection techniques ranging from arbitrarily chosen lags, lags chosen by three statistical criteria, and an extensive search of the lag space.

Thornton and Batten (1985) conclude:

> As a generalization … there appears to be no substitute for selecting a model specification criterion ex ante or for an extensive search of the lag space if one is to ensure that the causality test results are not critically dependent on the judicious (or perhaps fortuitous) choice of the lag structure.

With this background, in the present study Granger causality testing of NDVI-related data series pairs was conducted as follows:

- If hypothesis and the prior dynamic regression modelling used suggested a possible Granger link, tests were run based on model lags suggested from the results of the prior modelling

- If a Granger causality test set up as just described was positive at its default lag selection settings, that result was reported. If not, an extensive search of the lag space was carried out. That result was reported, positive or negative.

4.4.2. Results

Results are organised under the following headings:

4.4.2.1. Order of integration of series
4.4.2.2. Preparation of the pooled global NDVI series used
4.4.3. Relationship between climate variables and NDVI

4.4.2.1. Order of integration of series

As mentioned in Section 3. *Data and methods* of the ACPD paper**,** any two or more time series being assessed by time series regression analysis must be stationary in the first instance, or be capable of being transformed into a new stationary series (by differencing). A series is stationary if its properties (mean, variance, covariances) do not change with time (Greene 2012).

In the first instance, Augmented Dickey-Fuller (ADF) stationarity tests are calculated for each variable. Results and lag lengths chosen are given in Table 14.

The table shows that for this data from 1981, level of CO_2 and temperature are I(0), as they were for the data from 1959. This is not the case for first-derivative CO_2.

As can be seen, the ADF test result for first-derivative CO_2 for data from 1981 to 2012 of 0.0895 shows that first-derivative CO_2 approaches the statistical significance level of 0.05 required to be I(0), but does not reach it. In other words, for first derivative CO_2, the two I(0) and I(1) alternatives are close together.

For the reasons given by Zivot and Wang (2006) above, the order of integration of first-derivative CO_2 is therefore assessed by the wider range of tests for order of integration listed above, including the two tests nominated by Zivot and Wang (2006) as more sensitive when I(0) and I(1) alternatives are close together .

The results are given in Tables 15 to 17. All tests were run at their automatic setting for lags. For all tests, the null hypothesis is that the series is I(1), and the alternative is that it is I(0); except for the KPSS test (where the null hypothesis is that the series is I(0), and the alternative is that it is I(1)).

The ADF tests have been applied with an allowance for a drift and trend in the data, and the SIC was used to select degree of augmentation, k. For the KPSS tests the bandwidth, b, was selected using the Newey-West method, with the Bartlett kernel.

The significance level each test meets or surpasses is indicated by an asterisk in each column of the table.

Tables 15 to 17 show that the extra tests are not unanimous for the first-derivative CO_2 series.

The test using the alternative Schwartz or Akaike Information Criteria agree for two tests, DF-GLS and Ng-Perron. Here the I(0) statistical significance was between 0.05 and 0.1. For the other two tests, the Akaike Information Criterion gave lower probabilities: Elliott-Rothenberg-Stock Point Optimal between 0.05 and 0.1; ADF greater than 0.1. For the Schwartz Information Criterion the figures were $p<.01$ and statistical significance was between 0.05 and 0.1.

Finally, there were two tests – KPSS and Phillips-Perron – which used bandwidth criteria for the selection of an optimal lag length. Each of these tests characterised first-derivative CO_2 as I(0): statistical significance was at 0.05 and 0.01 respectively.

One of the tests recommended by Zivot and Wang (2006) for a series on the cusp of I(0) and I(1) – that of Elliot, Rothenberg, and Stock (1996) – gives a result for first difference CO_2 from 1981 to 2012 of I(0) at better than the 1% level; however, the similarly recommended Ng and Perron test gives I(0) at between the 5% and 10% level. Overall, three of the ten tests displayed probabilities of 5% or better, a further remaining six of between 5% and 10%. One of the 10 tests, the ADF under the Akaike Information Criterion, gave a result of greater than 10%.

It can be argued that the foregoing tests overall lean towards CO_2 from 1981 being I(0). To be conservative, however, in the following analyses first-derivative CO_2 is assessed separately both as I(0) and I(1).

4.4.2.2 Preparation of the pooled global NDVI series

The Normalized Difference Vegetation Index (NDVI) involves direct (satellite-derived) measurement of terrestrial plant activity.

To provide the full temporal span of the global NDVI data set used in this study, two NDVI series aggregated to global level were pooled. Each of the two series is derived from the same underlying spatially disaggregated Global Inventory Modeling and Mapping Studies (GIMMS) data set provided by the Global Land Cover Facility (GLCF) of the University of Maryland. This data is derived from imagery obtained from the Advanced Very High Resolution Radiometer (AVHRR) instrument carried by NOAA meteorological satellites. The two series enabled the longest time span of data aggregated at global level.

Globally aggregated GIMMS NDVI data from the Global Land Cover Facility (GLCF) site is available from 1980 to 2006. This dataset is referred to here as NDVIG. Spatially disaggregated GIMMS NDVI data from the Global Land Cover Facility (GLCF) site is available from 1980 to end 2013. An analogous global aggregation of this spatially disaggregated GIMMS NDVI data – from 1985 to end 2013 – was obtained from the Institute of Surveying, Remote Sensing and Land Information, University of Natural Resources and Life Sciences, Vienna. This dataset is abbreviated to NDVIV.

These two datasets were pooled as follows.

Figure 10 shows the appearance of the two series. Each series is Z-scored by the same common period of overlap (1985-2006). The extensive period of overlap can be seen, as can the close similarity in trend between the two series.

The figure also shows that the seasonal adjustment smoothings vary between the two series. Seasonality was removed for the NDVIV series using the 13 month moving average smoothing used throughout this paper. This required two passes using the 13 month moving average, which leads to a smoother result than seen for the NDVIG series.

Pretis and Hendry (2013) observe that pooling data (i) from very different measurement systems and (ii) displaying different behaviour in the sub-samples can lead to errors in the estimation of the level of integration of the pooled series.

The first risk of error (from differences in measurement systems) is overcome as both the NDVI series are from the same original disaggregated data set. The risk associated with the sub-samples displaying different behaviour and leading to errors in levels of integration is considered in the following section by assessing the order of each input series separately, and then the order of the pooled series.

Table 18 provides order of integration test results for the three NDVI series. The analysis shows all series are stationary (I(0)).

Because of the comparability of the NDVI series specified above, the series were pooled by adding Z-scored NDVIV data to the Z-scored NDVIG data at the point where the Z-scored NDVIG data ended in the last month of 2006.

4.4.3. Comparison of the pooled NDVI series with climate variables

The process we follow in this section is outlined below:

Relevant correlations involving first-derivative CO_2 characterised as I(1) are first assessed because of the near-stationarity of first-derivative CO_2 for the period 1981 to 2012.

As a check, we assess whether first-derivative CO_2 for the period from 1981 to 2012 has similar relationships to global surface temperature to those seen for the period 1959 to 2012.

We then explore remaining questions from our hypothesis concerning Granger causality and NDVI. These are firstly that there is Granger causality from first-derivative CO_2 to NDVI, and secondly from temperature to NDVI. Finally, we ask whether NDVI is Granger-causal for the difference between the level-of-CO_2 model for temperature and the observed temperature.

Where each series in a series pair is stationary, assessments are done for each of the questions above both by OLS dynamic regression modelling, and by Granger causality testing. The dynamic modelling is informative in itself, but as outlined above also informs correct model specification in terms of optimising model independent-variable lag for Granger causality testing (Thornton and Batten 1985).

The following information is relevant to each of the instances of OLS dynamic regression modelling which follow. As described in Section 4.1.3 *Time series analysis* of the ACPD paper, for OLS dynamic regression modelling, one must assess the extent (if any) of autocorrelation affecting the time series model. This is done by obtaining diagnostic statistics from an OLS regression. This regression shows, by means of the Breusch-Godfrey test for autocorrelation (up to order 20 – that is, including all monthly lags up to 20 months), .

If autocorrelation is found, it is taken to be a consequence of an inadequate specification of the temporal dynamics of the relationship being estimated. With this in mind, a dynamic model (Greene 2012) with sufficient lagged values of the dependent variable as additional independent variables is estimated.

If the autocorrelation can be removed, this will be shown by the use of the LMF test, supporting the use of this dynamic model specification.

4.4.3.1. First-derivative CO_2 as I(1)

Characterising first-derivative CO_2 as I(1) means dynamic regression modelling of the type presented above cannot be used. As in Section 4.1.4 *Granger causality analysis* of the ACPD paper, one can still assess the answer to the question: "Is there evidence of Granger causality between first-derivative CO_2 characterised as I(1) and relevant variables?" In this case the variables are global surface temperature and NDVI.

4.4.3.1.1 Does first-derivative CO_2 as I(1) display Granger causality of global surface temperature ?

In answering this question, because the TEMP series is stationary, but the first-difference CO_2 series is being treated as non-stationary (as integrated of order one, I(1)), the testing procedure is modified slightly. Once again, the levels of both series are used. This time a standard Vector Autoregressive (VAR) model is used. For each VAR model, the maximum lag length is determined, but then one additional lagged value of both TEMP and first-difference CO_2 is included in each equation of the VAR. However, the Wald test for Granger non-causality is applied only to the coefficients of the original k lags of first-difference CO_2. Toda and Yamamoto (1995) show that this modified Wald test statistic will still have an asymptotic distribution that is chi-square, even though the level of CO_2 is non-stationary.

Here the relevant Wald Statistic for the null hypothesis that is there is no Granger causality from first-derivative CO_2 as I(0) to temperature is shown in Table 19 to produce a Chi-Square of 32.79 (p=0.0001).

The high statistical significance in the p-value is strong evidence that first-derivative $CO_{2,}$ even treated as I(1), still displays Granger causality of temperature.

4.4.3.1.2 Does first-derivative CO_2 as I(1) display Granger causality of NDVI?

The identical steps to those in the previous section are used. Here the relevant Wald Statistic (Null hypothesis that is there is No Granger Causality from first-derivative CO_2 as I(1) to temperature) is shown in Table 20 to produce a Chi-Square of 3.184 ($p=0.9223$).

Hence in contrast with temperature, for the I(1) characterisation first-derivative CO_2 does *not* display Granger causality of NDVI.

4.4.3.2 Characterising first-derivative CO_2 as I(0)

4.4.3.2.1. Does first-derivative CO_2 as I(0) still display Granger causality of temperature for the 1981 to 2012 period?

A key finding earlier in the paper is that for the period 1959 to 2012, first-derivative CO_2 leads global surface temperature, is significant in an OLS dynamic regression model and is Granger-causal of global surface temperature. This section repeats that analysis (characterising first-derivative CO_2 as I(0)) for the period used for the NDVI data, 1981 to 2012.

Figure 11 displays the data series, and shows the similarity between the Z-scored curves.

Inspection of Table 21 shows that a highly statistically significant model has been established. First it shows that the temperature in a given period is strongly influenced by the temperature of closely preceding periods. Further it provides evidence that there is also a clear, highly statistically significant role in the model for first-derivative CO_2 for the period from 1981 to 2012 just as for the period from 1959 to 2012.

The next section assesses whether first-derivative CO_2 can be considered to display Granger causality for global surface temperature for the 1981 to 2012 period.

The relevant EViews output is from the Pairwise Granger Causality Test. Table 22 documents the following summary results: F-statistic 5.02 (p-value = 0.01). The forgoing statistic shows that the null hypothesis is rejected: in other words, there is strong evidence of Granger Causality from first-derivative CO_2 to global surface temperature for the shorter 1981 to 2012 period.

The table shows that the same first-derivative CO_2 which, characterised as I(1), displayed Granger causality for temperature (Table 19), characterised as I(0) also displays Granger causality for temperature.

4.4.3.3. Granger causality of NDVI

4.4.3.3.1 Does first-derivative CO_2 as I(0) display Granger causality of NDVI ?

Figure 12 shows Z-scored values for first-derivative CO_2 and NDVI. Considerable similarity between the signatures is seen.

An OLS dynamic regression model is set up using the procedure outlined in Section 3.2 above. Results are given in Table 23.

Inspection of Table 23 shows that a highly statistically significant model has been established. First it shows that as seen for temperature, the NDVI in a given period is strongly influenced by the NDVI of closely preceding periods. Further it provides evidence that there is also a statistically significant role in the model for first-derivative CO_2..

The next sections assess whether first-derivative CO_2 can be considered to display Granger causality of NDVI. Two assessments are made using different criteria for lag selection: the first using the Akaike Information Criterion; the second using the method of extensive search of the lag space (Thornton and Batten, 1985).

The relevant EViews output is from the Pairwise Granger Causality Test and Table 24 documents the following summary results: F-statistic 3.01 (p-value = 0.05). This statistic shows that using the Akaike Information Criterion for lag selection the null hypothesis is very slightly accepted: in other words, for the AIC there is (by a very narrow margin) an absence of evidence of Granger Causality from first-derivative CO_2 to NDVI.

Given the above result, what is the result from the extensive search method? The relevant EViews output is again from the Pairwise Granger Causality Test and Table 25 provides the following results: F-statistic 5.11 (p-value = 0.024).
This statistic shows that using the extensive search method for lag selection, the null hypothesis is rejected by a greater amount than for the AIC method, which reaches statistical significance: in other words, there is evidence of Granger Causality from first-derivative CO_2 to NDVI.

In summary, under the I(0) characterisation, first-derivative CO_2 displays Granger causality of NDVI, while under I(1), it does not.

4.4.3.3.2 Does TEMP display Granger causality of NDVI?

Figure 13 shows Z-scored values for first-derivative CO_2 and NDVI. With the exception of the period 2003-2004, considerable similarity between the signatures is seen.

An OLS dynamic regression model is set up using the procedure outlined in Section 3.2 above. Results are given in Table 26.

Inspection of Table 26 shows that a highly statistically significant model has been established. First it shows that, as seen for first-derivative CO_2, the NDVI in a given period is strongly influenced by the NDVI of closely preceding periods. Further it provides evidence that there is also a highly statistically significant role in the model for temperature.

The next section assesses whether temperature can be considered to display Granger causality of NDVI. The relevant EViews output is again from the Pairwise Granger Causality Test and is shown in Table 27.

Table 27 documents the following summary results: F-statistic 11.59 (p-value =1.00E-05). This statistic shows that the null hypothesis is rejected, by a highly statistically significant amount: in other words, there is strong evidence of Granger causality from temperature to NDVI.

4.4.3.3 Does NDVI display Granger causality of the difference between the level-of-CO_2 model for temperature and the observed temperature?

Figure 14 shows Z-scored values for f NDVI and the difference between the Z-scored level of atmospheric CO_2 (standing for the level-of-CO_2 model for temperature) and the Z-scored observed temperature. Considerable similarity between the signatures is seen.

An OLS dynamic regression model is set up using the procedure outlined in Section 3.2 above. Results are given in Table 28.

Inspection of Table 28 shows that a highly statistically significant model has been established. First it shows that the difference between the level-of-CO_2 model for temperature and the observed temperature in a given period is strongly influenced by that of closely preceding periods. Further it provides evidence that there is also a clear, highly statistically significant role in the model for NDVI.

With these results, Figure 15 is as for Figure 14 but with the NDVI series led indicated by the OLS dynamic regression modelling in Table 25.

A marked overall similarity between the two series is seen, both in core trend (as illustrated by polynomial curves of best fit) and in details of signature.

The next sections assess whether NDVI can be considered to display Granger causality of the difference between the level-of-CO_2 model for temperature and the observed temperature . As for first-derivative CO_2 and NDVI in Section 3.2.2.1 above, two assessments are made using different criteria for lag selection: the first using the Akaike Information Criterion; the second using the method of extensive search of the lag space (Thornton and Batten, 1985).

The relevant EViews output is from the Pairwise Granger Causality Test and Table 29 documents the following summary results: F-statistic 1.03 (p-value = 0.36).
This statistic shows that using the Akaike Information Criterion for lag selection, the null hypothesis is rejected: in other words, for the AIC there is an absence of evidence of Granger causality from NDVI to the difference between the level-of-CO_2 model for temperature and the temperature observed.

The relevant EViews output from the extensive search method is again from the Pairwise Granger Causality Test and Table 30 documents the following summary results: F-statistic 1.81 (p-value = 0.03). This statistic shows that using the extensive search method for lag selection, the null hypothesis is rejected: in other words, there is evidence of Granger causality from first-derivative CO_2 to NDVI.
The way in which the search reveals the statistically significant lag is depicted visually in Figure 16. Note the statistical significance of results of tests based on lags 14 to 16.

Considering the results of Section 4.4 overall, the following analysis is made.

Even considering first-derivative CO_2 as possibly being I(1) for the period 1981 to 2012, it is believed that there is sufficient redundancy in the range of data series and relationships used in the NDVI section to answer the question as to whether vegetation at global scale causes the difference between the linear CO_2-temperature model and observed temperature.

The redundancy comes about as follows. The Granger-causality with Toda-Yamamoto procedure results in Tables 16 and 17 show that, while first-derivative CO_2 as I(1) does not display Granger causality of NDVI, first-derivative CO_2 as I(1) does display Granger causality of temperature. And temperature characterised as I(0) – as it unambiguously is shown to be (Table 11) – is shown to display Granger causality of NDVI (Table 14).

So whichever level of integration first-difference CO_2 is characterised as, adequate dynamic-regression and Granger-causality linkages are in place for the flow of causality from first-derivative CO_2 and temperature to NDVI.

It is also shown, in this case without ambiguities concerning the I(0) nature of series, that NDVI displays Granger causality of the difference between the linear CO_2-temperature model and observed temperature.

In conclusion, it is considered that the results in this section show a Granger-causal chain from first-derivative CO_2 and temperature to NDVI, and from NDVI to the difference between the linear CO_2-temperature model and observed temperature.

5 Discussion

Firstly it is noted that the results in this paper show that there are clear links - at the highest standard of non-experimental causality: that of Granger causality – between all of first- and second-derivative CO_2, global surface temperature, SOI and NDVI.

Given the extensiveness of these Granger causality results, it is worth at the outset revisiting the question of the strength of the causality evidence which arises from Granger causality analysis.

As discussed in Section 3. *Data and Methods* of the ACPD paper, Stern and Kander (2011) observe that Granger causality is not identical to causation in the classical philosophical sense, but it does demonstrate the likelihood of such causation or the lack of such causation more forcefully than does simple contemporaneous correlation. However, where a third variable, z, drives both x and y, x might still appear to drive y though there is no actual causal mechanism directly linking the variables. Any such third variable must have some plausibility.

Turning to the plausibility of any (currently missing) third variable driving both climate and vegetation, it is noted that this third variable must have energetics on a scale of an order analogous to those of global vegetation and climate.

The ocean is one such candidate in terms of energetics, but it is noted that its dynamics are of far lower frequency – are more damped – than those of observed for global vegetation and climate.

It is noted that until a plausible third candidate is found, Granger causality evidence for causality is effectively equivalent to experimental evidence for causality.

Furthermore, there is support for the present Granger causality findings from evidence at the level of the causality "gold standard", the experiment – direct manipulation of variables in terms of subject and control group categories. This evidence comes from the results of direct experimentation on plants Dieleman et al. (2012) outlined in Section 2.2 above. This experimental evidence for separate CO_2 and temperature effects on plant growth is consistent with that for the effects of CO_2 and temperature on NDVI from the present Granger causality analysis.

Concerning statistical significance, the results show that relationships between first- and second-derivative CO_2 and climate variables are present for all the time scales studied: that is, including temporal start points situated as long ago as 1500. In the instances where time series analysis accounting for autocorrelation could be successfully conducted, the results were always statistically significant. For the further instances (commencing in 1500) the data was not amenable to time series analysis due to the strongly smoothed nature of the temperature data making removal of the autocorrelation impossible (see Section 4.3). Nonetheless the scale of the non-corrected correlations observed were of the same order of magnitude as those of the instances that were able to be corrected for autocorrelation.

Turning to the time scales over which these effects are observed, taken as a whole the results clearly suggest that the mechanism observed is long term, and not, for example, a creation of the period of the steepest increase in anthropogenic CO_2 emissions which commenced in the 1950s (IPCC, 2013).

A further notable finding is the major role of immediate past instances of the dependent variable in its own present state. This was found in all cases where time series models could be prepared, and was true for temperature, SOI and NDVI. This was not to detract from the role of first- and second-derivative CO_2 – in all relevant cases, they were significant in the models as well.

A number of points arise from the NDVI results. First, as mentioned in the Introduction, the standard notion of the greenhouse effect suggested by general circulation climate models (GCMs) (IPCC, 2013) has it that global temperature will rise almost linearly with an increasing level of global atmospheric CO_2. As also mentioned in the Introduction, in recent years global surface temperature has trended below that predicted by these models.

The results in Section 4.4 show that the NDVI signature closely fits this difference between GCM models and the observed temperature, and displays Granger causality of it. As the NDVI time series represents the changing levels of activity of the terrestrial biosphere, this result provides strong evidence that the terrestrial biosphere mechanism is the cause of the departure of temperature from that predicted by the level-of-CO_2 mechanism alone.

The above said, these results are supportive of the anthropogenic global warming hypothesis. Firstly, the results show that variations in atmospheric carbon dioxide influence surface temperature. First-derivative atmospheric CO_2 is shown to drive global temperature and the results deepen the support for CO_2 affecting climate, in that second-derivative CO_2 is shown to drive the SOI. Lastly, the results show that the

NDVI signature fits the difference between the global surface temperature observed trend and that suggested by the standard AGW hypothesis / radiative forcing mechanism. This fit provides evidence that the terrestrial biosphere mechanism is the cause of this departure of temperature from that predicted by the standard AGW hypothesis / level-of-CO_2 forcing mechanism alone. In other words, the results provide evidence for the case that the final warming achieved is the result not of one mechanism – the physical greenhouse gas radiative mechanism embodied in the standard anthropogenic global warming hypothesis – but of the interaction of that mechanism with a second, residing in the terrestrial biosphere.

(If so, it is notable that CO_2 is having two different influences on climate through two quite different mechanisms – the first, a radiative one, with CO_2 as a greenhouse gas, the second as a result of plants utilising CO_2 as a resource!)

Research questions arising from these results include those of (i) the conditions under which the current increase in plant biomass can be expected to continue, and (ii) the range of alternative expected future trajectories for human greenhouse gas emissions. Obviously the combinations of the extremes of these ranges may produce quite different future climate trend outcomes.

If plants are the agents of these phenomena, then plants would require mechanisms to: (i) detect rate of change of relevant environmental cues, including CO_2; and (ii) because of the evidence provided in this paper for the major role of immediate past instances of the dependent variable in its own present state, provide a capacity for "memory", for periods not only of months but of years.

This section reviews evidence from plant research relevant to both of these points.

First we consider the mechanism of plant responsiveness to atmospheric CO_2. With regard to responsiveness in general (for review see Volkov and Markin 2012), it has been shown that plants can sense mechanical, electrical and electromagnetic stimuli, gravity, temperature, direction of light, insect attack, chemicals and pollutants, pathogens, water balance, etc. Looking more closely at responsiveness to CO_2, for the stomata of plants – the plant components which regulate gas exchange including CO_2

and oxygen at the plant surface – extensive research (for example, Maser et al., 2003) has shown that a network of signal transduction mechanisms integrates water status, hormone responses, light, CO_2 and other environmental conditions to regulate stomatal movements in leaves for optimization of plant growth and survival under diverse conditions.

While we have not been able to find studies measuring such sensitivity to stimuli in rate of change and acceleration terms – that is, in terms of first- and second-derivatives – such sensitivity is widely present in animal systems (for example in the form of acceleration detectors for limb control (Vidal-Gadea et al. 2010)). Indeed Spitzer and Sejnowski (1997) argue that rather than occurring rarely, such differentiation and other computational processes are present and potentially ubiquitous in living systems, including at the single-celled level where a variety of biological processes – concatenations of chemical amplifiers and switches – can perform computations such as exponentiation, differentiation, and integration.

Plants with the ability to detect the rate of change of resources – especially scarce resources – would have a clear selective advantage. First and second derivatives, for example, are each leading indicators of change in the availability of a given resource. Leading indicators of change in CO_2 would enable a plant's photosynthetic apparatus to be ready in advance to harvest CO_2 when, for seasonal or other reasons, increasing amounts of it become available. In this connection, it is noteworthy that second-derivative capacity would provide greater advance warning than first.

Has CO_2 ever been such a scarce resource? According to Ziska (2008) plants evolved at a time of high atmospheric carbon dioxide (4-5 times present values), but concentrations appear to have declined to relatively low values during the last 25-30 million years. Therefore, it has been argued that for the last c. 20 million years, terrestrial plant evolution has been driven by the optimisation of the use of its scarce 'staple food', CO_2.

.

In this connection, a review by Franks et al. (2013) points out that plants have been equipped with most, if not all, of the fundamental physiological characteristics governing net CO_2 assimilation rate (e.g. stomata, chloroplasts, leaves, roots, hydraulic systems) for at least 370 million years. Given that atmospheric CO_2 has fluctuated at least five to ten times its current ambient concentration over the same period, it is possible, even likely, that a generalised long-term net CO_2 assimilation rate versus atmospheric CO_2 relationship evolved early in the history of vascular plants.

What mechanism in plants might provide memory capacity? Studies of vernalization – the capacity of some plants to flower in the spring only after exposure to prolonged cold – show that some plants must not only have the capacity to *sense* cold exposure but also have a mechanism to *measure the duration* of cold exposure and then *store* that information (Amasino 2004). In some species this "memory" of vernalization can be maintained for up to 330 days (Lang 1965).

With the foregoing points, the plant model seems worthy of further consideration. Many of the questions of mechanism seem ideal for laboratory experiments.

6. Conclusion

Prior to the present paper, observational studies at global level and experimental studies at laboratory level had provided evidence that plants might be a factor in explaining the difference between the level-of-CO_2 model for temperature and the observed temperature.

At global level, this evidence was only correlational. Questions of cause and effect were not settled, and the potential scale of any effect had not been quantified.

Concerning quality of evidence, the laboratory evidence was considered to be at "gold standard" – that of the experiment (involving the direct manipulation of variables in terms of subject and control groups). The laboratory experiments showed that responsiveness of plants to temperature and CO_2 was present which could fully enable plants to be a factor in explaining the climate model/temperature difference. What could not be known from laboratory experiments was whether or not these attributes of individual plants could sum coherently to produce discernable results at global scale.

The present results using Granger causality throw light on the above questions. They show that the responsiveness of plants to temperature and CO_2 seen at laboratory level is clearly discernable at global level.

The results showing this are two-fold. The first is the coherent presence of a CO_2 signature in a measure of the aggregate of global terrestrial photosynthetic activity, the NDVI. The second is the similarly coherent presence of the NDVI signature in the difference between the level-of-CO_2 model for temperature and the observed temperature.

It is believed that the results in this paper provide strong evidence that the global climate is the result of the combination of two mechanisms – one, a physical mechanism based on the level of atmospheric CO_2, the other a mechanism embodied in the terrestrial biosphere and based on the rate of change of CO_2.

References

Adams, J. M. and Piovesan, G.: Long series relationships between global interannual CO_2 increment and climate: Evidence for stability and change in role of the tropical and boreal-temperate zones. Chemosphere, 59, 1595 – 1612, 2005.

Amasino, R.: Vernalization, competence, and the epigenetic memory of winter. Historical perspective essay. The Plant Cell, 16, 2553–2559, 2004.

Attanasio, A. and Triacca, U.: Detecting human influence on climate using neural networks based Granger causality," Theor. Appl. Climatol., 103,1-2,103-107, 2011.

Attanasio, A.: Testing for linear Granger causality from natural/anthropogenic forcings to global temperature anomalies Theor. Appl. Climatol. 110:281–289, 2012.

Banerjee, A. Dolado, J. Galbraith, J.W. and Hendry, D.F.: Co-integration, error-correction, and the econometric analysis of non-stationary data. Oxford University Press, Oxford, 1993.

Barichivich, J., Briffa, K. R., Myneni, R. B., Osborn, T. J., Melvin, T. M., Ciais, P., Piao, S., and Tucker, C.: Large-scale variations in the vegetation growing season and annual cycle of atmospheric CO2 at high northern latitudes from 1950 to 2011, Glob. Change Biol., 19, 3167–3183, 2013.

Bacastow, R. B.: Modulation of atmospheric carbon dioxide by the southern oscillation, Nature, 261, 116–118, 1976.

Canty, T., Mascioli, N. R. Smarte, M. D. and Salawitch R. J. An empirical model of global climate – part 1: A critical evaluation of volcanic cooling, Atmos. Chem. Phys. 13 3997–4031 2013.

Bellenger, H., Guilyardi, E., Leloup, J., Lengaigne, M., and Vialard, J.: ENSO representation in climate models: from CMIP3 to CMIP5, Clim. Dynam., 42, 1999-2018, 2014.

Chen, X. Tung, K. Varying planetary heat sink led to global-warming slowdown and acceleration. Science 345, 897, DOI: 10.1126/science.1254937, 2014.

Cox P.M., Pearson D., Booth B.B., Friedlingstein P., Huntingford C., Jones C.D., and Luke C.M. : Sensitivity of tropical carbon to climate change constrained by carbon dioxide variability, Nature, 494, 341–344, 2013.

Denman, K.L., G. Brasseur, G. Chidthaisong, A. Ciais, P. P.M. Cox, P.M. Dickinson, R.E. Hauglustaine, D. Heinze, Holland, C.E, Jacob, D. Lohmann, U. Ramachandran, S. da Silva Dias, P.L. Wofsy, S.C. and Zhang, X.: Couplings between changes in the climate system and biogeochemistry, Climate Change 2007: The physical science basis. Contribution of working group I to the fourth assessment report of the intergovernmental panel on climate change [Solomon, S. Qin,D. Manning, M. Chen, Z. MMarquis, M. Averyt, K.B. Tignor, M. and Miller, H.L. (eds.)]. Cambridge University Press, Cambridge, United Kingdom and New York, NY, USA, 2007.

Dickey, D.A. and Fuller, W.A.: Distribution of the estimators for autoregressive time series with a unit root, Journal of the American Statistical Association, 74, 427–431, 1979.

Dickey, D. A. and Fuller, W. A.: Likelihood ratio statistics for autoregressive time series with a unit root, Econometrica, 49, 1057–1072, 1981.

Dieleman, W. I. J. Vicca, S. Dijkstra, F. A. Hagedorn, F. Hovenden, M. J. Larsen, K. S. Morgan, J. A.,Volder, A. Beier, C. Dukes, J. S. King, J. Leuzinger, S. Linder, S. Luo, Y. Oren, R. De Angelis, P. Tingey, D. Hoosbeek, M. R. and Janssens, I. A. Simple additive effects are rare: a quantitative review of plant biomass and soil process responses to combined manipulations of CO_2 and temperature, Glob. Change Biol., 18, 2681–2693, 2012.

Elliott, G., Rothenberg T. J.. and Stock J. H.: Efficient tests for an autoregressive unit root, Econometrica, 64, 813-836, 1996.

Folland C.K., Colman A.W., Smith D.M., Boucher O., Parker D.E., and Vernier J.P. : High predictive skill of global surface temperature a year ahead, Geophys. Res. Lett., 40, 761–767, 2013.

Foster, G. and Rahmstorf, S.: Global temperature evolution 1979–2010, Environ. Res. Lett., 6, 044022, 2011.

Franks P.J., Adams M.A., Amthor J.S., Barbour M.M., Berry J.A., Ellsworth D.S., Farquhar G.D., Ghannoum O., Lloyd J., McDowell N., Norby R. J., Tissue D. T., and von Caemmerer S.: Sensitivity of plants to changing atmospheric CO2 concentration: from the geological past to the next century, New Phytol., 197, 1077–1094, 2013.

Frisia, S., A. Borsato, N. Preto, and F. McDermott.: Late Holocene annual growth in three Alpine stalagmites records the influence of solar activity and the North Atlantic Oscillation on winter climate, Earth and Planetary Science Letters, 216, 411–424, 2003.

Fyfe, J. C., Gillett, N.P, and Zwiers, F. W.: Overestimated global warming over the past 20 years, Nature Climate Change, 3 767–769, 2013.

Fyfe J.C and Gillett, N.P.: Recent observed and simulated warming, Nature Climate Change, 4, 150-151, 2014.

Granger, C.W.J.: Investigating causal relations by econometric models and cross-spectral methods, Econometrica, 37, 3, 424-438, 1969.

Greene, W. H.: Econometric Analysis (7th ed.), Prentice Hall, Boston, 2012.

Gribbons, B. and Herman, J.: True and quasi-experimental designs. Practical assessment, research and evaluation, 5, http://PAREonline.net/getvn.asp?v=5&n=14, 1997.

Guemas V., Doblas-Reyes F.J., Andreu-Burillo I. and Asif M.: Retrospective prediction of the global warming slowdown in the past decade, Nature Climate Change, 3, 649–653, 2013.

Guilyardi, E., Bellenger H., Collins M., Ferrett S., Cai, W., and Wittenberg A.: A first look at ENSO in CMIP5, Clivar. Exch., 17, 29–32, 2012.

Ghosh, S. and Rao, C. R. eds.: Design and Analysis of Experiments, Handbook of Statistics, 13, North-Holland, 1996.

Hansen, J., Kharecha, P., and Sato, M.: Climate forcing growth rates: doubling down on our Faustian bargain, Environ. Res. Lett., 8, 2013.

Hazewinkel, M., ed.: Finite-difference calculus, Encyclopedia of Mathematics, Springer 2001.

Hidalgo, F. and Sekhon, J.: Causality. In Badie, B., Berg-Schlosser, D., and Morlino, L. (Eds.), International encyclopedia of political science, 204-211, 2011.

Holbrook, N.J. Davidson, J. Feng, M. Hobday, A.J. Lough, J.M. McGregor, S. and Risbey, J.S.: El niño-southern oscillation, In: A marine climate change impacts and adaptation report card for Australia 2009, (Eds. Poloczanska, E.S. Hobday, A.J. and Richardson, A.J.) NCCARF Publication, 05/09, 2009.

Hume D.: An enquiry into human understanding (1751) cited in: Hidalgo, F., & Sekhon, J.: Causality. In Badie, B., Berg-Schlosser, D. & Morlino, L. (Eds.) International encyclopedia of political science, 204-211, 2011.

Hyndman, R.J.: Moving averages. in Lovirc, M. (ed.), International encyclopedia of statistical science. 866-869 Springer, New York, 2010.

Imbers, J., Lopez, A., Huntingford, C., and Allen M. R.: Testing the robustness of the anthropogenic climate change detection statements using different empirical models, J. Geophys. Res.-Atmos., 118, 3192–3199, 2013.

IPCC, Climate Change 2007: The physical science basis. Contribution of working group I to the fourth assessment report of the intergovernmental panel on climate change [IPCC, Qin, D. Manning, M. Chen, Z. Marquis, M. Averyt, K.B. Tignor, M. and Miller, H.L. (eds.)]. Cambridge University Press, Cambridge, United Kingdom and New York, NY, USA, 2007.

IPCC, 2013: Climate Change 2013: The Physical Science Basis. Contribution of Working Group I to the Fifth Assessment Report of the Intergovernmental Panel on Climate Change [Stocker, T.F., D. Qin, G.-K. Plattner, M. Tignor, S.K. Allen, J. Boschung, A. Nauels, Y. Xia, V. Bex and P.M. Midgley (eds.)]. Cambridge University Press, Cambridge, United Kingdom and New York, NY, USA, 1535 pp.

Katz, R.W.: Sir Gilbert Walker and a connection between El Niño and statistics, Statistical Science, 17, 97–112, 2002.

Kaufmann R.K., Kauppi H., and Stock J.H.: Emissions, concentrations, and temperature: a time series analysis, Clim. Change, 77, 249–278, 2006.

Keeling R-F, Piper S-C, Bollenbacher A-F, Walker S-J (2009) Carbon Dioxide Research Group, Scripps Institution of Oceanography (SIO), University of California, La Jolla, California USA 92093-0444, Feb 2009., http://cdiac.ornl.gov/ftp/trends/co2/maunaloa.co2, last access: 14 July 2014.

Kiviet, J.F.: On the rigour of some misspecification tests for modelling dynamic relationships, Review of Economic Studies*, 53*, 241-261, 1986.

Kodra, E., Chatterjee, S., and Ganguly, A.R.: Exploring Granger causality between global average observed time series of carbon dioxide and temperature, Theoretical and Applied Climatology, 104, 3-4, 325-335, 2011.

Kopp, G. and Lean, J. L.: A new, lower value of total solar irradiance: evidence and climate significance. Geophys. Res. Lett., 38, 2011.

Körner, C.: Plant CO_2 responses: an issue of definition, time and resource supply, New Phytologist, 172, 393– 411, 2006.

Kosaka, Y. and Shang-Ping, X.: Recent global-warming hiatus tied to equatorial Pacific surface cooling, Nature, doi:10.1038/nature12534, 2013.

Kuo C., Lindberg C., and Thomson D.J.: Coherence established between atmospheric carbon dioxide and global temperature, Nature, 343, 709–714, 1990.
Kwiatkowski, D.; Phillips, P. C. B.; Schmidt, P. and Shin, Y.: Testing the null hypothesis of stationarity against the alternative of a unit root, Journal of Econometrics 54, 159–178, 1992.

Lang, A.: A physiology of flower initiation, in Encyclopedia of plant physiology, Ruhland, W.,and Berlin (eds.) , Springer-Verlag, 1965.

Le Quéré, C., Peters, G. P., Andres, R. J., Andrew, R. M., Boden, T., Ciais, P., Friedlingstein, P., Houghton, R. A., Marland, G., Moriarty, R., Sitch, S., Tans, P., Arneth, A., Arvanitis, A., Bakker, D. C. E., Bopp, L., Canadell, J. G., Chini, L. P., Doney, S. C.,Harper, A., Harris, I., House, J. I., Jain, A. K., Jones, S. D., Kato, E., Keeling, R. F., Klein Goldewijk, K., Körtzinger, A., Koven,C., Lefèvre, N., Omar, A., Ono, T., Park, G.-H., Pfeil, B., Poulter, B., Raupach, M. R., Regnier, P., Rödenbeck, C., Saito, S.,Schwinger, J., Segschneider, J., Stocker, B. D., Tilbrook, B., vanHeuven, S., Viovy, N., Wanninkhof, R., Wiltshire, A., Zaehle, S.,and Yue, C.: Global carbon budget 2013, Earth Syst. Sci. Data, 6, 235–263, 2014

Lean, J.L. and Rind, D.H.: How natural and anthropogenic influences alter global and regional surface temperatures: 1889 to 2006, Geophys. Res. Lett., 35, 2008.

Lean, J. L. and Rind , D.H.: How will Earth's surface temperature change in future decades? Geophys. Res. Lett. 36, L15708, 2009.

Lean, J.L. and Rind, D.H.: How natural and anthropogenic influences alter global and regional surface temperatures: 1889 to 2006, Geophys. Res. Lett., 35, 2008.

Lockwood M.: Recent changes in solar outputs and the global mean surface temperature. III. Analysis of contributions to global mean air surface temperature rise. Proceedings of the Royal Society, Mathematical Physical and Engineering Sciences, 464, 1387–1404, 2008.

Maser, P., Leonhardt, N., and Schroeder, J.I.: The clickable guard cell: electronically linked model of guard cell signal transduction pathways. In: The Arabidopsis Book, http://www-biology.ucsd. edu/labs/schroeder/clickablegc.html. 2003.

Meehl, G. A. Arblaster, J.M. Fasullo, J.T.1, Hu, A, and Trenberth, K.E.: Model-based evidence of deep-ocean heat uptake during surface-temperature hiatus periods, Nature Climate Change, DOI: 10.1038/NCLIMATE1229

Meehl, G. A., C. Covey, T. Delworth, M. Latif, B. McAvaney, J. F. B. Mitchell, R. J. Stouffer, and K. E. Taylor: The WCRP CMIP3 multi-model dataset: A new era in climate change research,Bulletin of the American Meteorological Society, **88**, 1383-1394. 2007. (CMIP3) Multi-Model Mean20c3m/sresa1, http://climexp.knmi.nl/selectfield_CO2, last access 10 June 2014

Moberg, A., D.M. Sonechkin, K. Holmgren, N.M. Datsenko and W. Karlén.: Highly variable Northern Hemisphere temperatures reconstructed from low- and high-resolution proxy data, Nature, 433, 7026, 613-617, 2005.

Morice, C.P., Kennedy, J.J., Rayner, N.A. and Jones, P.D.: Quantifying uncertainties in global and regional temperature change using an ensemble of observational estimates: the HadCRUT4 dataset. Journal of Geophysical Research, **117**, 2012. D08101, doi:10.1029/2011JD017187 http://www.metoffice.gov.uk/hadobs/hadcrut4/data/download.html, last access 25 August 2014.

Ng, S. and Perron, P.: Lag length selection and the construction of unit root tests with good size and power, Econometrica, 69, 1519-1554, 2001.

Pankratz , A.: Forecasting with Dynamic Regression Models. Wiley, New York, 386 pp. 1991.

Phillips, P.C.B. and Perron, P.: Testing for a unit root in time series regression, Biometrika, 75, 335–346, 1988.

Robertson, A. Overpeck, J. Rind, D. Mosley-Thompson, D. E. Zielinski, G. Lean, J. Koch, D. Penner, J. Tegen, I. & Healy, R.: Hypothesized climate forcing time series for the last 500 years, Journal of Geophysical Research,106, D14, 2001.

Running, S. W., Nemani, R. R., Heinsch, F. A., Zhao, M., Reeves, M. C., and Hashimoto, H.: A continuous satellite-derived measure of global terrestrial primary production, BioScience, 54, 547–560, 2004

Sato, M., Hansen, J. E., McCormick, M. P. & Pollack, J. B. Stratospheric aerosol optical depths, 1850–1990. J. Geophys. Res., 98, 22987–22994, 1993. http://data.giss.nasa.gov/modelforce/strataer/tau.line_2012.12.txt, last access 10 August 2014.

Spitzer, N. C., and Sejnowski, T. J.: Biological information processing: bits of progress, Science, 277, 1060–1061, 1997.

Stahle, D.W., R.D. D'Arrigo, P.J. Krusic, M.K. Cleaveland, E.R. Cook, R.J. Allan, J.E. Cole, R.B. Dunbar, M.D. Therrell, D.A. Gay, M.D. Moore, M.A. Stokes, B.T. Burns, J. Villanueva-Diaz and Thompson, L.G.: Experimental dendroclimatic reconstruction of the Southern Oscillation, Bull. American Meteorological Society, 79, 2137-2152, 1998.

Steger, U., Achterberg, W., Blok, K., Bode, H., Frenz, W., Gather, C., Hanekamp, G., Imboden, D., Jahnke, M., Kost, M., Kurz, R., Nutzinger, H.G. & Ziesemer, T.: Sustainable development and innovation in the energy sector. Berlin: Springer. 2005.

Stern, D.I. and Kander, A.: The role of energy in the industrial revolution and modern economic growth, CAMA Working Paper Series, Australian National University, 2011.

Stern, D.I and Kaufmann, R.K.: Anthropogenic and natural causes of climate change, Climatic Change, 122, 257-269, DOI 10.1007/s10584-013-1007-x, 2014.

Sun, L. and Wang, M.: Global warming and global dioxide emission: an empirical study, Journal of Environmental Management, 46, 327–343, 1996.

Thornton, D. L. and Batten, D. S.: Lag-length selection and tests of Granger causality between money and income. Journal of Money, Credit and Banking, 17, 164-178, 1985.

Toda, H. Y. and Yamamoto, T.: Statistical inferences in vector autoregressions with possibly integrated processes, Journal of Econometrics, 66, 225-250. 1995.

Troup, A.J.: The Southern Oscillation, Quarterly Journal of Royal Meteorological Society, 91, 490-506, 1965. https://www.longpaddock.qld.gov.au/seasonalclimateoutlook/southernoscillationindex/soidatafiles/MonthlySOI1887-1989Base.txt, last access 25 August 2014.

Triacca, U.: Is Granger causality analysis appropriate to investigate the relationship between atmospheric concentration of carbon dioxide and global surface air temperature?, Theoretical and Applied Climatology, 81, 133–135, 2005.

Tucker, C.J., J. E. Pinzon, M. E. Brown, D. Slayback, E. W. Pak, R. Mahoney, E. Vermote and N. El Saleous, An extended AVHRR 8-km NDVI data set compatible with MODIS and SPOT vegetation NDVI data, International Journal of Remote Sensing, 26, 4485-5598, 2005. http://climexp.knmi.nl/select.cgi?id=someone@somewhere&field=ndvi, last access 30 July 2014.

Tung, K.-K. and Zhou, J.: Using data to attribute episodes of warming and cooling in instrumental records, PNAS, 110, 2058-2063, 2013.

Vidal-Gadea, A.G., Jing, X.J., Simpson, D., Dewhirst, O., Kondoh, Y., & Allen, R.: Coding characteristics of spiking local interneurons during imposed limb movements in the locust, J. Neurophysiol, 103, 603–15, 2010.

Volkov, A.G. and Markin V.S.: Phytosensors and phytoactuators. In: Alexander G. Volkov Editor: Plant Electrophysiology Signaling and Responses 369pp Springer-Verlag, Berlin, 2012.

Wang, C., Deser, C., Yu, J.-Y., DiNezio, P., and Clement, A.: El Niño–Southern Oscillation (ENSO): a review, in: Coral Reefs of the Eastern Pacific, Glynn, P. Manzello, D., and Enochs, I., Springer Science, 2012.

Wang, W., Ciais, P., Nemani, R. R., Canadell, J. G., Piao, S., Sitch, S., White, M. A., Hashimoto, H., Milesi, C., and Myneni, R. B.: Variations in atmospheric CO_2 growth rates coupled with tropical temperature, Proc. Natl. Acad. Sci. USA, 110, 13061–13066, 2013.

Zhang, Y., Guanter, L., Berry J.A., Joiner, J., van der Tol, C., Huete, A., Gitelson, A.,Voigt. M., and Köhler P.: Estimation of vegetation photosynthetic capacity from space-based measurements of chlorophyll fluorescence for terrestrial biosphere models, Global Change Biology, doi: 10.1111/gcb.12664, 2014.

Zhou, J. and Tung, K.: Deducing multidecadal anthropogenic global warming trends using multiple regression analysis, Journal of the Atmospheric Sciences, 70, 1-8, 2013.

Ziska, L. H.: Rising atmospheric carbon dioxide and plant biology: the overlooked paradigm. In: Controversies in Science and Technology, From Climate to Chromosomes. Eds. Kleinman, D.L., Cloud-Hansen, K.A. *et al.* Liebert, Inc., New Rochele: 379-400, 2008.

Table 1. Lag of first-derivative CO_2 relative to surface temperature series for global, tropical, northern hemisphere and southern hemisphere categories

	Lag in months of first-derivative CO_2 relative to global surface temperature category
hadcrut4SH	-1
hadcrut4Trop	-1
HadCRUT4_nh	-3
hadcrut4Glob	-2

Table 2. Lag of FIRST-DERIVATIVE CO_2 relative to surface temperature series for global, tropical, northern hemisphere and southern hemisphere categories, each for three time-series sub-periods

Temperature category	Time period	Lag of first-derivative CO_2 relative to global surface temperature series
NH	1959.87 to 1976.46	-6
NH	1976.54 to 1993.21	-6
Global	1959.87 to 1976.46	-4
SH	1959.87 to 1976.46	-3
Global	1976.54 to 1993.21	-2
Tropical	1959.87 to 1976.46	0
Tropical	1976.54 to 1993.21	0
Tropical	1993.29 - 2012.37	0
Global	1993.29 - 2012.37	0
NH	1993.29 - 2012.37	0
SH	1976.54 to 1993.21	0
SH	1993.29 - 2012.37	0

Table 3: Augmented Dickey–Fuller (ADF) test for tests for unit roots stationarity in monthly data 1969 to 2012 for global surface temperature, level of atmospheric CO_2 and first-derivative CO_2

	ADF statistic*	p-value	Test interpretation
TEMP	-6.942	0.000	Stationary
FIRST-DERIVATIVE CO_2	-4.646	0.001	Stationary
CO_2	-1.222	0.904	Non-stationary

* The Dickey-Fuller regressions allowed for both drift and trend; the augmentation level was chosen by minimizing the Schwarz Information Criterion.

Table 4. OLS dynamic regression between first-derivative atmospheric CO_2 and global surface temperature for monthly data for the period 1959 - 2012, with autocorrelation taken into account

Independent variable/s [1]	Dep-endent variable [1]	Independent variable regression coefficients	Indep-endent variable P-value	Whole model adjusted R-squared	Whole model P-value	LM test for autocorr-elation [2]
Led2mx13mma 1stderiv CO_2	TEMP	0.097	<0.00001	0.861	6.70E-273	0.144
Led1mTEMP		0.565	<0.00001			
Led2mTEMP		0.306	<0.00001			

[1] Z-scored
[2] Whole model: LM test for autocorrelation up to order 12 - Null hypothesis: no autocorrelation

Table 5. Pairwise correlations (correlation coefficients (R)) between selected climate variables

	2x13mmafirstderiv CO_2	Hadcrut4Global	3x13mma2ndderivCO_2
Hadcrut4Global	**0.7**	1	
3x13mma2ndderivCO_2	0.06	-0.05	1
13mmaReverseSOI	0.25	0.14	**0.37**

Table 6. Pairwise correlations (correlation coefficients (R)) between selected climate variables, phase-shifted as shown in the table

	Led2m2x13mmafirstderivCO2	Hadcrut4Global	Led4m3x13mma2ndderivCO2
Hadcrut4Global	**0.71**	1	

Led4m3x13mma2ndderivCO2	0.23	0.09	1
13mmaReverseSOI	0.16	0.14	**0.49**

Table 7. Pairwise correlations (correlation coefficients (R)) between selected climate variables, phase-shifted as shown in the table

	ZLed2m2x13mma2ndderiv CO_2	**ZReverseLongPaddock SOI**
ZReverseLongPaddockSOI	0.28	1.00
ZLed3m13mmafirstderivhadcrut4 global	0.35	0.41

Table 8. OLS dynamic regression between second-derivative atmospheric CO_2 and reversed Southern Oscillation Index for monthly data for the period 1959 - 2012, with autocorrelation taken into account

Independent variable/s [1]	**Dep-endent variable [1]**	**Independent variable regression coefficients**	**Indep-endent variable P-value**	**Whole model adjusted R-squared**	**Whole model P-value**	**LM test for autocorr-elation [2]**
Led3m2x13mma 1stderivCO_2	ReverseSOI	0.07699	<0.011	0.478	1.80E-89	0.214
Led1mReverseSOI		0.456	<0.00001			
Led2mreverseSOI		0.272	<0.00001			

[1] Z-scored
[2] Whole model: LM test for autocorrelation up to order 12 - Null hypothesis: no autocorrelation

Table 9. OLS dynamic regression between first-derivative global surface temperature and reversed Southern Oscillation Index for monthly data for the period 1877-2012, with autocorrelation taken into account

Indep-endent variable/s [1]	**Dep-endent variable [1]**	**Independent variable regression coefficients**	**Indep-endent variable P-value**	**Whole model adjusted R-squared**	**Whole model P-value**	**LM test for autocorr-elation [2]**
Led3m12mma1stderivTEMP	ReverseSOI	0.140	<0.00001	0.466	3.80E-221	0.202

Led1mReverseSOI		0.465	<0.00001			
Led2mReverseSOI		0.210	<0.00001			

[1] Z-scored
[2] Whole model: LM test for autocorrelation up to order 3 - Null hypothesis: no autocorrelation

Table 10: Augmented Dickey–Fuller (ADF) test for stationarity for monthly data 1959 to 2012 for second-derivative CO_2 and sign-reversed SOI

	ADF statistic	**p-value**	**Test interpretation**
Second-derivative CO_2	-10.077	0.000	Stationary
Sign-reversed SOI	-6.681	0.000	Stationary

Table 11. VAR Residual Serial Correlation LM Tests component of Granger-causality testing of relationship between second-derivative CO2 and SOI. Initial 2-lag model

Lag order	**LM-Stat**	**P-value***
1	10.62829	0.0311
2	9.71675	0.0455
3	2.948737	0.5664
4	9.711391	0.0456
5	10.67019	0.0305
6	37.13915	0
7	1.268093	0.8668

*P-values from chi-square with 4 df.

Table 12. VAR Residual Serial Correlation LM Tests component of Granger-causality testing of relationship between second-derivative CO2 and SOI. Preferred 3-lag model

Lag order	LM-Stat	P-value*
1	1.474929	0.8311
2	4.244414	0.3739
3	2.803332	0.5913
4	13.0369	0.0111
5	8.365221	0.0791
6	40.15417	0
7	1.698265	0.791

*P-values from chi-square with 4 df.

Table 13. Correlations (R) between paleoclimate CO_2 and temperature estimates 1500-1940

	Temperature (speliothem)	Temperature (tree ring)
Level of CO_2 (ice core)	0.369	0.623
1st deriv. CO_2 (ice core)	0.558	0.721

Table 14: ADF test results for time series based on automatic Schwarz Information Criterion (SIC) lag length selection

	ADF	
		Prob.
1stderivCO_2	Lag Length: 15 (Automatic - based on SIC, maxlag=16)	0.0895
Temp	Lag Length: 1 (Automatic - based on SIC, maxlag=16)	0.0000
NDVI	Lag Length: 1 (Automatic - based on SIC, maxlag=16	0.0000
Climate model/temperature difference	Lag Length: 1 (Automatic - based on SIC, maxlag=16)	0.0000

Table 15. Order of integration test results for first-derivative CO_2 for monthly data from 1981-2012. The Akaike information criterion (AIC) was used to select an optimal maximum lag length (k) for the variables in the test. The null

hypothesis for the tests is non-stationarity, except for the KPSS test for which the null hypothesis is stationarity.

	Test critical values	ADF	DF-GLS	Elliott-Rothenberg-Stock Point Optimal	Ng-Perron - Modified ERS Point Optimal statistic
Test statistic		-2.75	-2.73	5.77	6.11
	1% level	-3.98	-3.48	3.97	4.03
	5% level	-3.42	-2.90	5.63	5.48
	10% level	-3.13	-2.58*	6.89*	6.67*

(1) Significant at <1% level

Table 16. Order of integration test results for first-derivative CO_2 for monthly data from 1981-2012. The Schwartz information criterion (SIC) was used to select an optimal maximum lag length (k) for the variables in the test. The null hypothesis for the tests is non-stationarity, except for the KPSS test for which the null hypothesis is stationarity.

	Test critical values	ADF	DF-GLS	Elliott-Rothenberg-Stock Point Optimal	Ng-Perron - Modified ERS Point Optimal statistic
Test statistic		-3.183	-2.73	3.193	6.105
	1% level	-3.984	-3.476	3.971*	4.03
	5% level	-3.422	-2.898	5.625	5.48
	10% level	-3.134*	-2.585*	6.886	6.670*

Table 17. Order of integration test results for first-derivative CO_2 for monthly data from 1981-2012. Tests use bandwidth criteria for lag selection. The null hypothesis for the tests is non-stationarity, except for the KPSS test for which the null hypothesis is stationarity.

	Test critical values	KPSS does not use AIC or SIC	Phillips-Perron does not use AIC or SIC
Test statistic		0.07	-3.60
	1% level	0.22*	-3.98
	5% level	0.15	-3.42*
	10% level	0.12	-3.13

Table 18. Order of integration test results for NDVI series for monthly data from 1981-2012. The Schwartz Information Criterion (SIC) was used to select an optimal maximum lag length in the tests.

NDVI Series	**Null Hypothesis: the series has a unit root**	**Probability of unit root**
NDVIV	Lag Length: 16 (Automatic - based on SIC, maxlag=16)	0.0122
NDVIG	Lag Length: 1 (Automatic - based on SIC, maxlag=15)	7.23e-14
NDVIGV	Lag Length: 1 (Automatic - based on SIC, maxlag=16)	4.18E-16

Table 19. Pairwise Granger causality tests for first-derivative CO_2 and temperature

Null Hypothesis:	**Lags suggest-ed by AIC**	**Number of lags imple-mented**	**Total observ-ations**	**Included observ-ations**	**Chi-sq**	**df**	**Prob.**	**Interpret-ation**
TEMP does not GC 1stderivCO_2	8	Add one more lag to allow for fact that 1stderiv CO_2 is characterised I(1), but don't include extra lag in GC test (Toda and Yamamoto ,1 995)	378	369	7.39	8	p=0.4962	TEMP does not GC 1stderivCO_2
1stderivCO_2 does not GC TEMP	8		378	369	32.79	8	p=0.0001	1stderivCO_2 does GC TEMP

Table 20. Pairwise Granger causality tests for first-derivative CO_2 characterised as I(1) and NDVI

Null Hypothesis:	Lags suggest-ed by AIC	Number of lags imple-mented	Total observ-ations	Included observ-ations	Chi-sq	df	Prob.	Interpret-ation
NDVI does not GC 1stderivCO_2	8	Add one more lag to allow for fact that 1stderiv CO_2 is characterised I(1), but don't include extra lag in GC test (Toda and Yamamoto ,1995)	378	369	3.184	8	p=0.9223	NDVI does not GC 1stderivCO_2
1stderivCO_2 does not GC NDVI	8		378	369	12.312	8	p=0.1378	1stderivCO_2 does not GC NDVI

Table 21. OLS dynamic regression between first-derivative atmospheric CO_2 and global surface temperature for monthly data for the period 1981-2012, with autocorrelation taken into account

Independent variable/s [1]	Dep-endent variable [1]	Independent variable regression coefficients	Indep-endent variable P-value	Whole model adjusted R-squared	Whole model P-value	LM test for autocorr-elation [2]
Twox13mma1stderivCO_2	**TEMP**	0.107	0.00077	0.770	4.00E-118	0.445
Led1mTEMP		0.545	<0.00001			
Led2mTEMP		0.293	<0.00001			

[1] Z-scored
[2] Whole model: LM test for autocorrelation up to order 20 - Null hypothesis: no autocorrelation

Table 22. Pairwise Granger causality tests for first-derivative atmospheric CO_2 and global surface temperature

Null Hypothesis:	Criterion for number of lags selected	Number of lags imple-mented	Observ-ations	F-Statistic	Probab-ility	Interpretation of statistically significant probabilities
TEMP does not Granger Cause 1stderivCO_2	AIC	2	373	2.88	0.06	
1stderivCO_2 does not Granger Cause TEMP				5.02	0.01	1stderivCO_2 Granger Causes TEMP

Table 23. OLS dynamic regression between first-derivative atmospheric CO_2 and NDVI for monthly data for the period 1981 - 2012, with autocorrelation taken into account

Indep-endent variable/s [1]	Dep-endent variable [1]	Independent variable regression coefficients	Indep-endent variable P-value	Whole model adjusted R-squared	Whole model P-value	LM test for autocorr-elation [2]
Twox13mma 1stderivCO_2	NDVI	0.094	0.01103	0.549	3.74E-64	0.092
Led1mNDVI		0.765	<0.00001			
Led2mNDVI		−0.075	0.15231			

[1] Z-scored
[2] Whole model: LM test for autocorrelation up to order 20 - Null hypothesis: no autocorrelation

Table 24. Pairwise Granger causality tests for first-derivative CO_2 and NDVI: lag selection by AIC

Null Hypothesis:	Criterion for number of lags selected	Number of lags imple-mented	Observations	F-Statistic	Probability	Interpretation of statistically significant probabilities
NDVI does not Granger Cause 1stderivCO_2	AIC	2	373	1.25	0.29	Not significant
1stderivCO_2 does not Granger Cause NDVI				3.01	0.0504	Not significant

Table 25. First-derivative CO_2 displays Granger causality of NDVI: lag selection by extensive search

Null Hypothesis:	Criterion for number of lags selected	Number of lags imple-mented	Observations	F-Statistic	Probability	Interpretation of statistically significant probabilities
NDVI does not Granger Cause 1stderivCO_2	Result of extensive search of lag space	1	374	0.87	0.352	
1stderivCO_2 does not Granger Cause NDVI				5.11	0.024	1stderivCO_2 Granger Causes NDVI

Table 26. OLS dynamic regression between global surface temperature and NDVI for monthly data for the period 1981 - 2012, with autocorrelation taken into account

Indep-endent variable/s [1]	Dependent variable [1]	Independent variable regression coefficients	Independent variable P-value	Whole model adjusted R-squared	Whole model P-value	LM test for autocorrelation [2]
TEMP	NDVI	0.215	<0.00001	0.574	1.18E-68	0.536
Led1mNDVI		0.720	<0.00001			
Led2mNDVI		−0.122	0.01874			

[1] Z-scored
[2] Whole model: LM test for autocorrelation up to order 20 - Null hypothesis: no autocorrelation

Table 27. Pairwise Granger causality tests for temperature and NDVI

Null Hypothesis:	Criterion for number of lags selected	Number of lags imple-mented	Observations	F-Statistic	Probability	Interpretation of statistically significant probabilities
NDVI does not Granger Cause TEMP	AIC	2	373	3.18	0.043	NDVI Granger Causes TEMP
TEMP does not Granger Cause NDVI				11.59	1.00E-05	TEMP Granger Causes NDVI

Table 28. OLS dynamic regression between NDVI and the difference between the observed level of atmospheric CO_2 and global surface temperature for monthly data for the period 1981 - 2012, with autocorrelation taken into account

Indep-endent variable/s [1]	Depen-dent variable [1]	Independent variable regression coefficients	Independent variable P-value	Whole model adjusted R-squared	Whole model P-value	LM test for autocorrelation [2]
Led17mNDVI	Climate model/temperature difference	0.069	0.00795	0.557	1.36E-62	0.874
Led1mClimate model/temperature difference		0.490	<0.00001			
Led2mClimate model/temperature difference		0.265	<0.00001			

[1] Z-scored
[2] Whole model: LM test for autocorrelation up to order 20 - Null hypothesis: no autocorrelation

Table 29. Pairwise Granger causality tests for NDVI and the difference between the observed level of atmospheric CO_2 and global surface temperature: Akaike information criterion used to select lag

Null Hypothesis:	Criterion for number of lags selected	Number of lags imple-mented	Observations	F-Statistic	Probability	Interpretation of statistically significant probabilities
Climate model/temperature difference does not Granger Cause Led17mNDVI	AIC	2	356	2.35	0.10	Not significant
Led17mNDVI does not Granger Cause climate model/temperature difference				1.03	0.36	Not significant

Table 30. Pairwise Granger causality tests for NDVI and the difference between the observed level of atmospheric CO_2 and global surface temperature: extensive search of the lag space

Null Hypothesis:	Criterion for number of lags selected	Number of lags imple-mented	Observations	F-Statistic	Probability	Interpretation of statistically significant probabilities
Climate model/temperature difference does not Granger Cause Led17mNDVI	Result of extensive search of lag space	15	343	0.83	0.65	
Led17mNDVI does not Granger Cause climate model/temperature difference				1.81	0.03	Led17mNDVI Granger Causes climate model/temperature difference

Figure 1. Monthly data: global surface temperature (HADCRUT4 dataset) (red dotted curve) and an IPCC mid-range scenario model (CMIP3, SRESA1B scenario) run for the IPPC fourth assessment report (IPCC, 2007) (blue curve), each expressed in terms of Z scores to aid visual comparison (see Sect. 1).

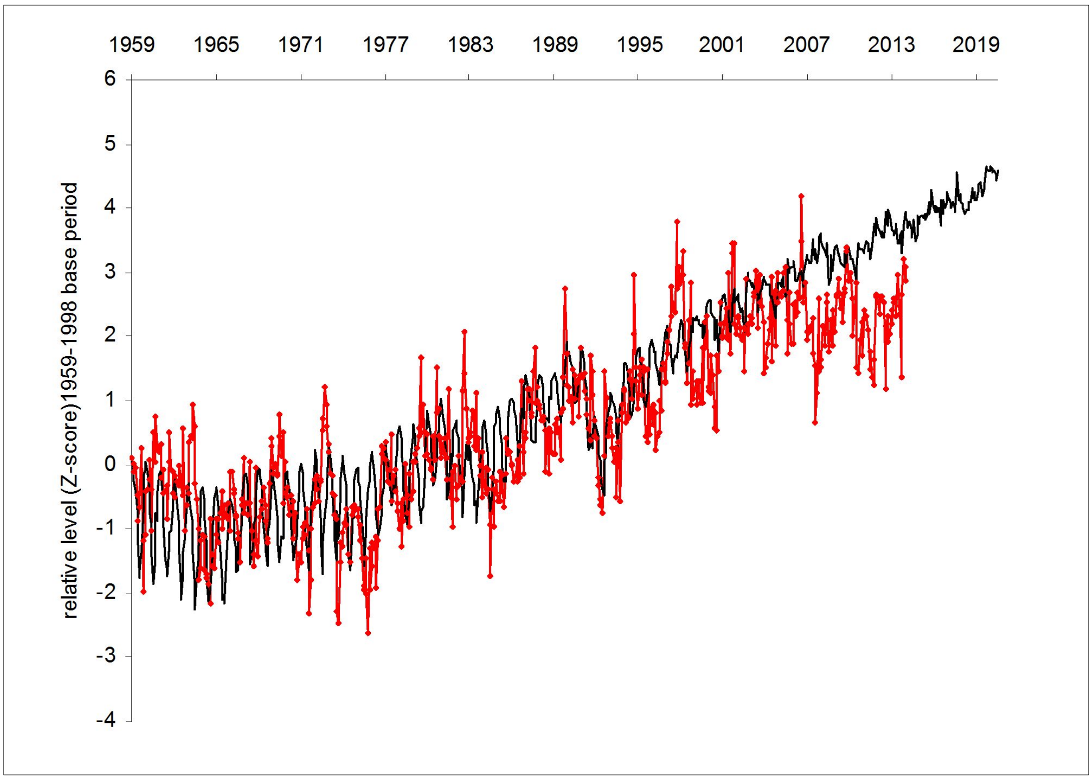

Figure 2. Z scored monthly data: global surface temperature (green dashed curve) compared to an IPCC mid-range scenario model (CMIP3, SRESA1B scenario) run for the IPCC fourth assessment report (IPCC, 2007) (blue curve) and also showing the trend in first-derivative atmospheric CO_2 (smoothed by two 13 month moving

averages) (red dotted curve). To show their core trends for illustrative purposes the three series are fitted with 5th order polynomials.

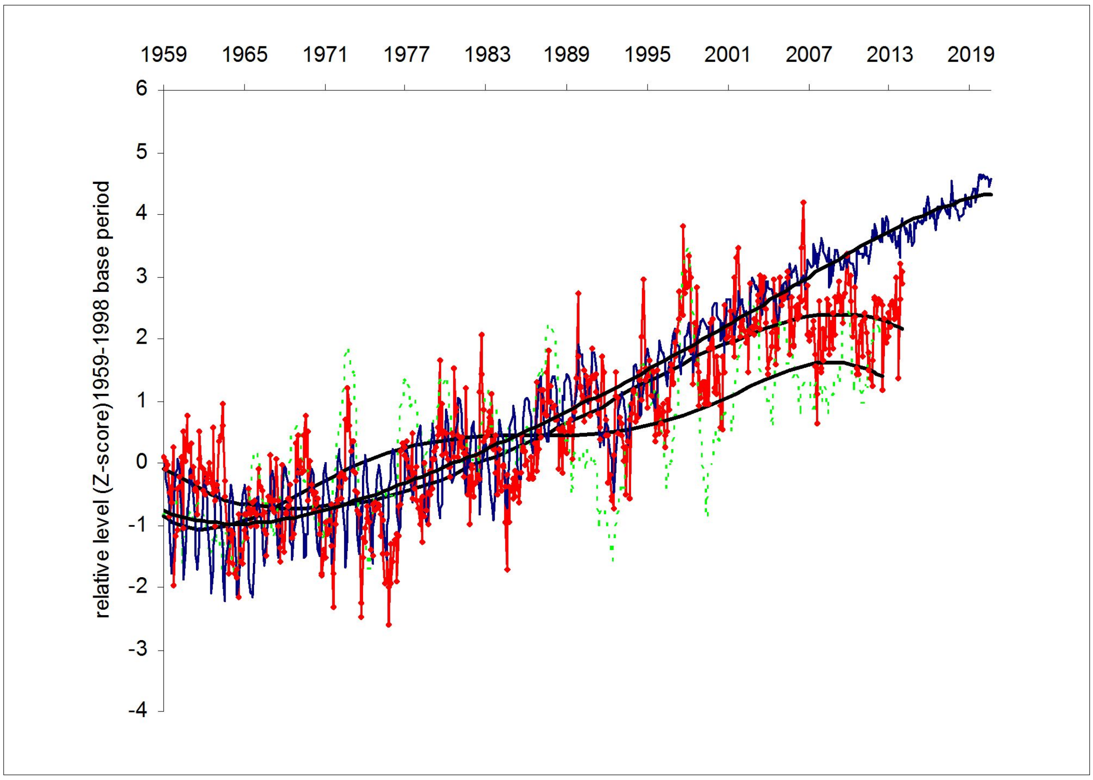

Figure 3. Z scored monthly data: global surface temperature (red curve) compared to first-derivative atmospheric CO_2 smoothed by two 13 month moving averages (black dotted curve).

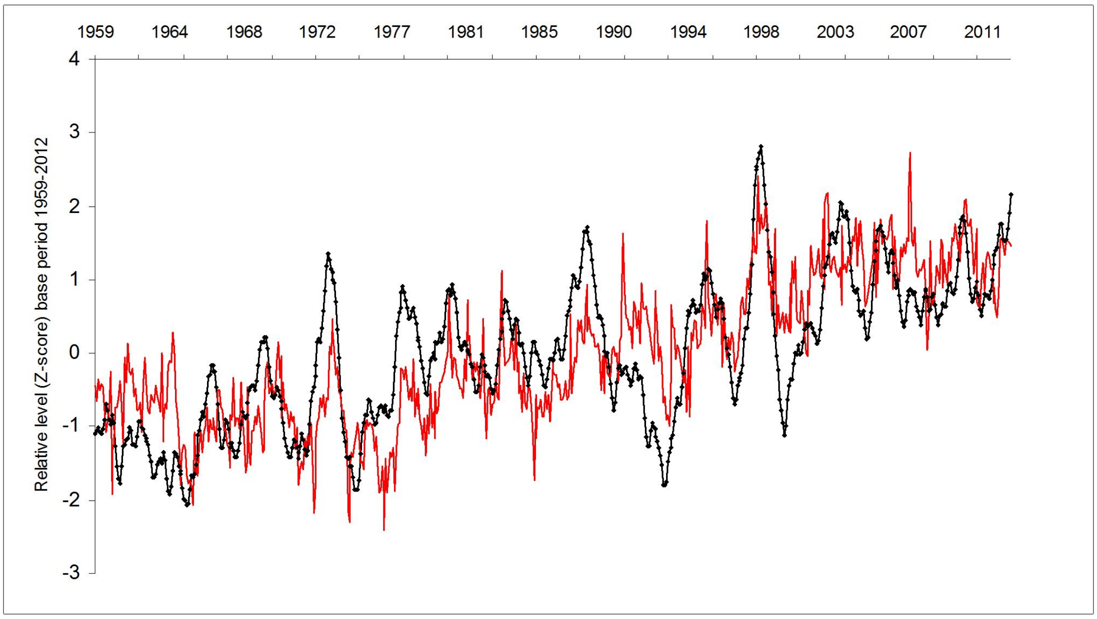

Figure 4. Correlograms of first-derivative CO_2 with surface temperature for global (turquoise curve with crosses), tropical (blue curve with triangles), Northern Hemisphere (purple curve with boxes) and Southern Hemisphere (black curve with diamonds) categories

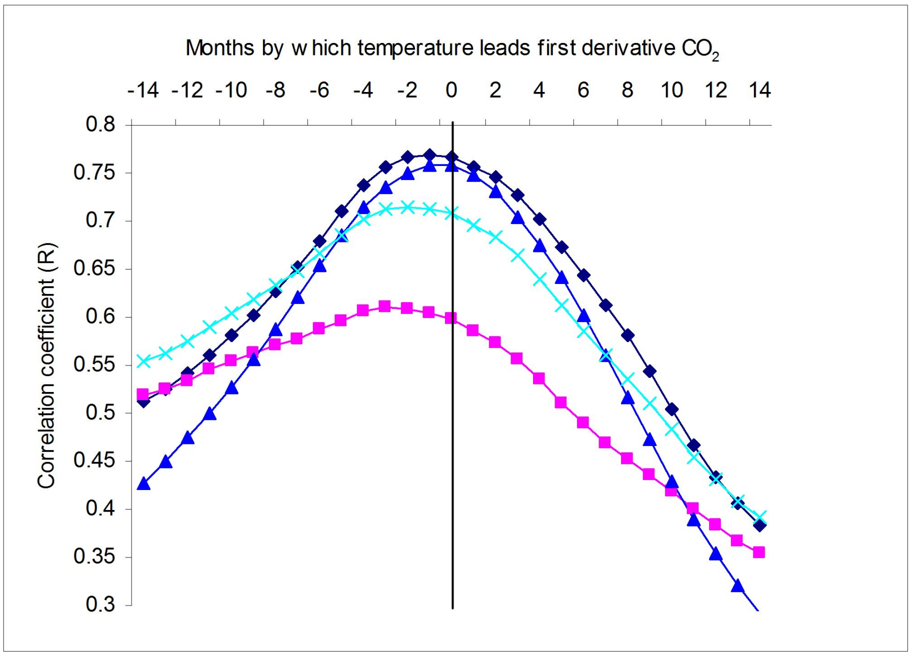

Figure 5. Correlograms of first-derivative CO_2 with surface temperature for global, tropical, Northern Hemisphere and Southern Hemisphere categories, each for three time-series sub-periods.

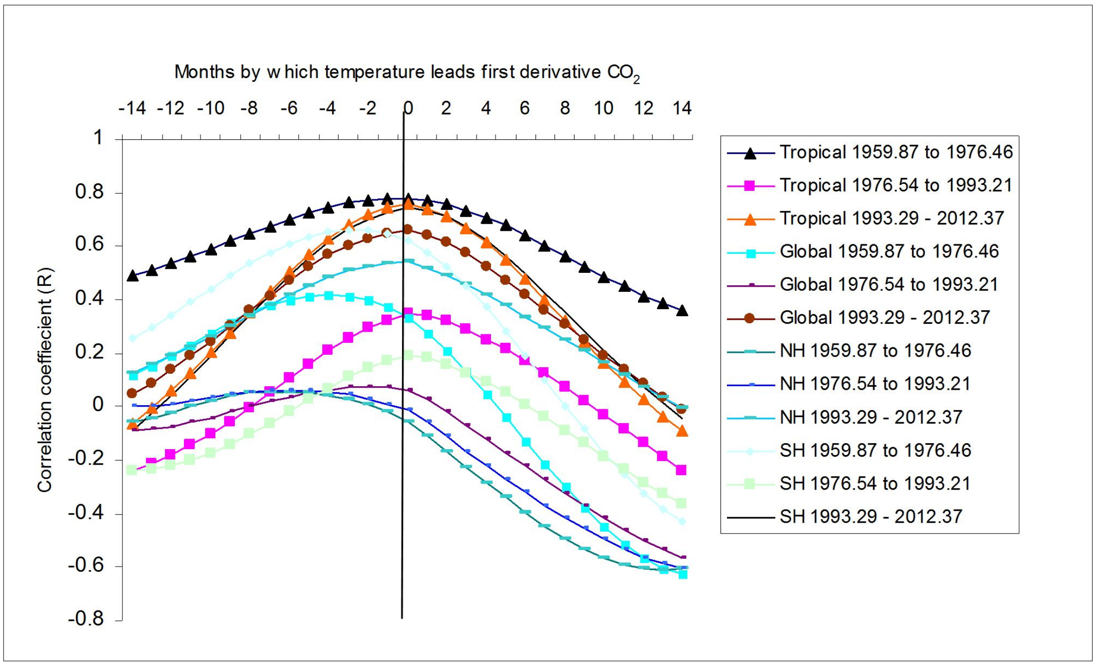

Figure 6. Z scored monthly data: global surface temperature (red curve) and first-derivative atmospheric CO_2 smoothed by two 13 month moving averages (black dotted curve) (left-hand scale); sign-reversed SOI smoothed by a 13 month moving average (blue dashed curve) and second-derivative atmospheric CO_2 smoothed by three 13 month moving averages (green barred curve) (right-hand scale)

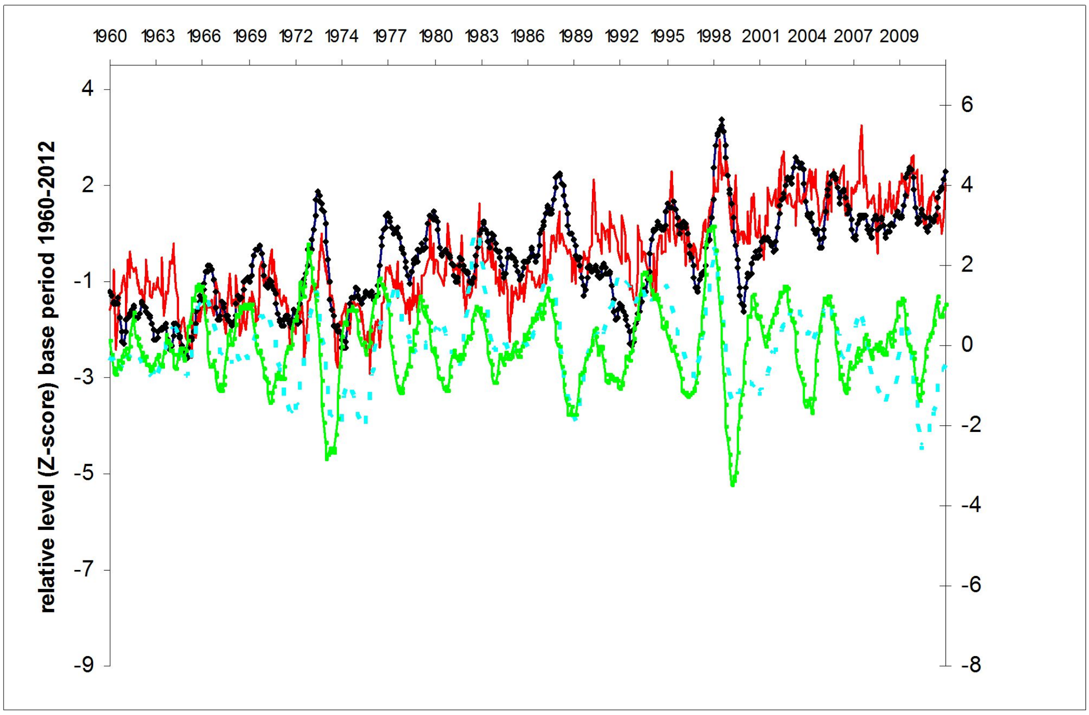

Figure 7. Z scored monthly data from 1960 to 2012: sign-reversed SOI (unsmoothed and neither led nor lagged) (dotted black curve); second-derivative CO_2 smoothed by a 13 month × 13 month moving average and led relative to SOI by 2 months (green

dashed curve); and first-derivative global surface temperature smoothed by a 13 month moving average and led by 3 months (red curve).

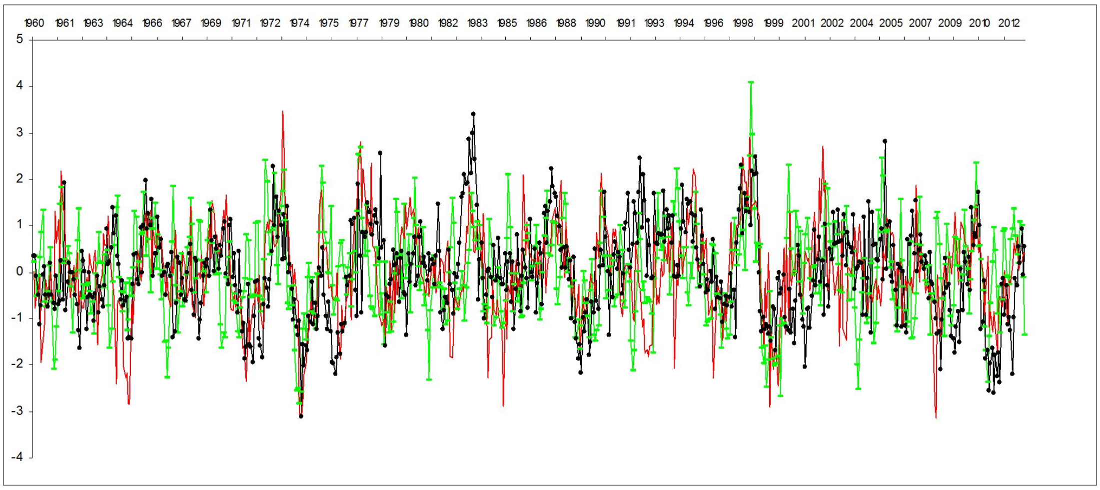

Figure 8. Z scored monthly data from 1877 to 2012: sign-reversed SOI (unsmoothed and neither led nor lagged) (red curve); and first-derivative global surface temperature smoothed by a 13 month moving average and led relative to SOI by 3 months (black dotted curve)

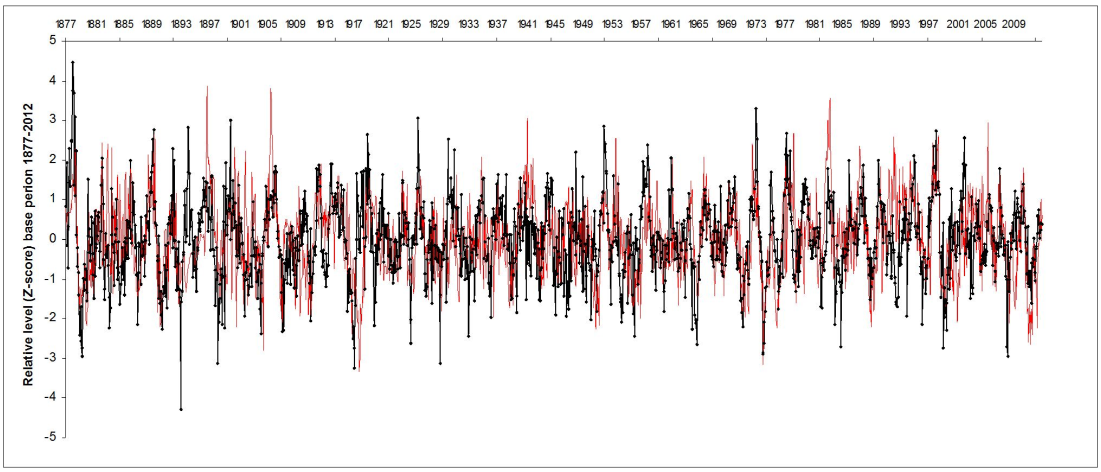

Figure 9. *Z* scored annual data: paleoclimate time series from 1500: ice core level of CO_2 (blue curve), level of CO_2 transformed into first-derivative form (green barred

curve); and temperature from speliothem (red dashed curve) and tree ring data (black boxed curve).

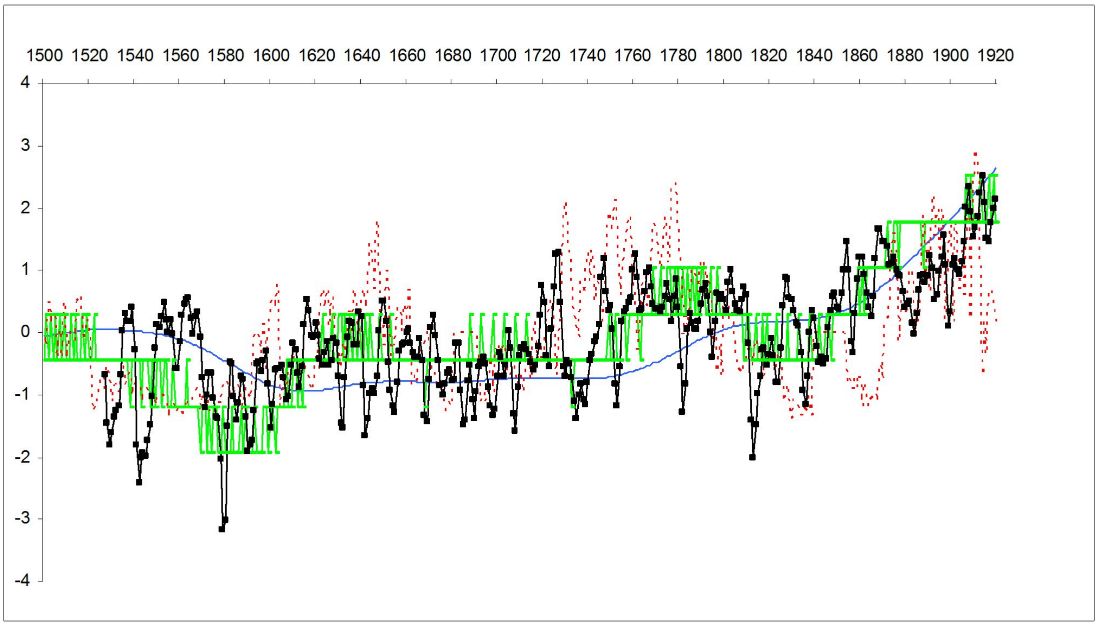

Figure 10: *Z* scored monthly data: NDVIG (black dotted curve) compared to NDVIV (red curve).

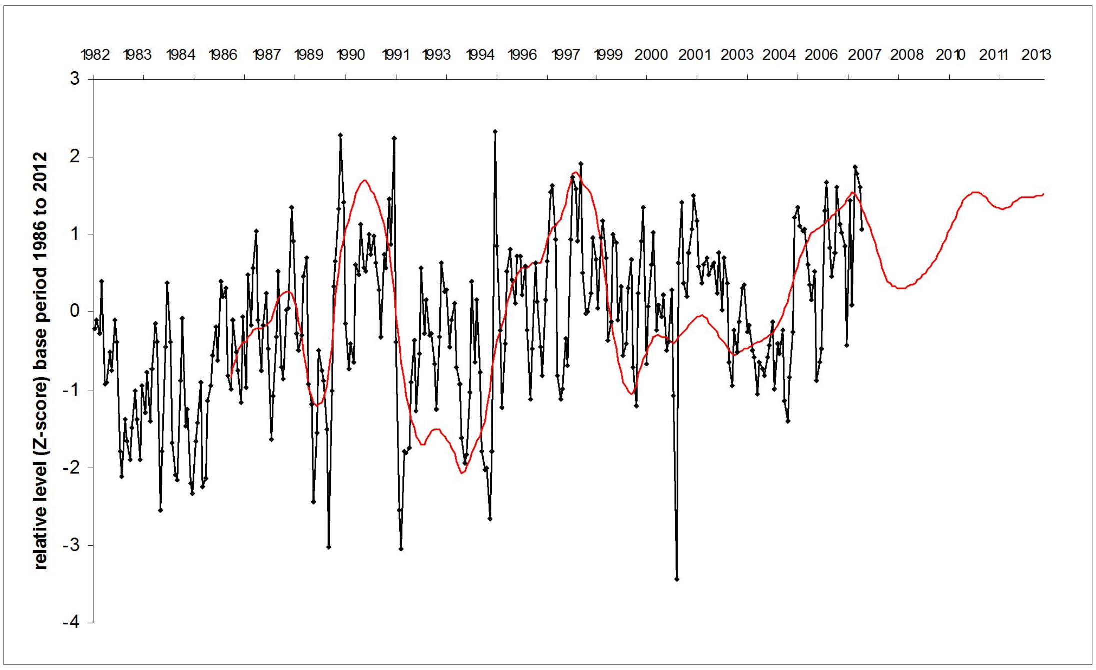

Figure 11. *Z* scored monthly data: global surface temperature (red curve) compared to first-derivative atmospheric CO_2 smoothed by two 13 month moving averages (black dotted curve).

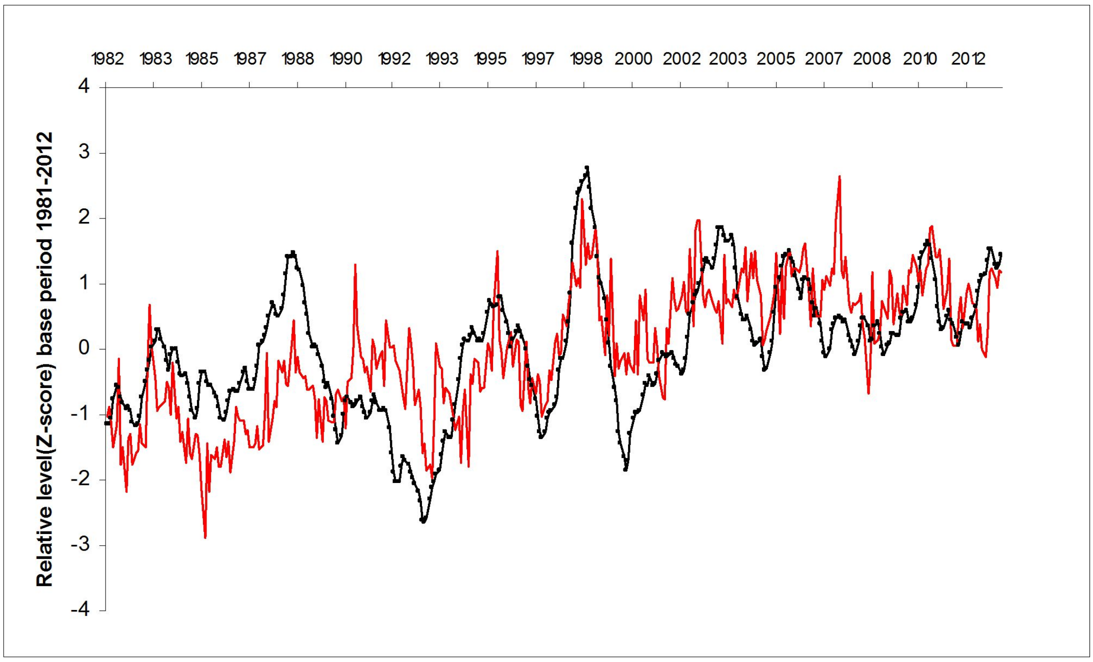

Figure 12. Z scored monthly data: NDVI (red curve) compared to first-derivative atmospheric CO_2 smoothed by two 13 month moving averages (black dotted curve).

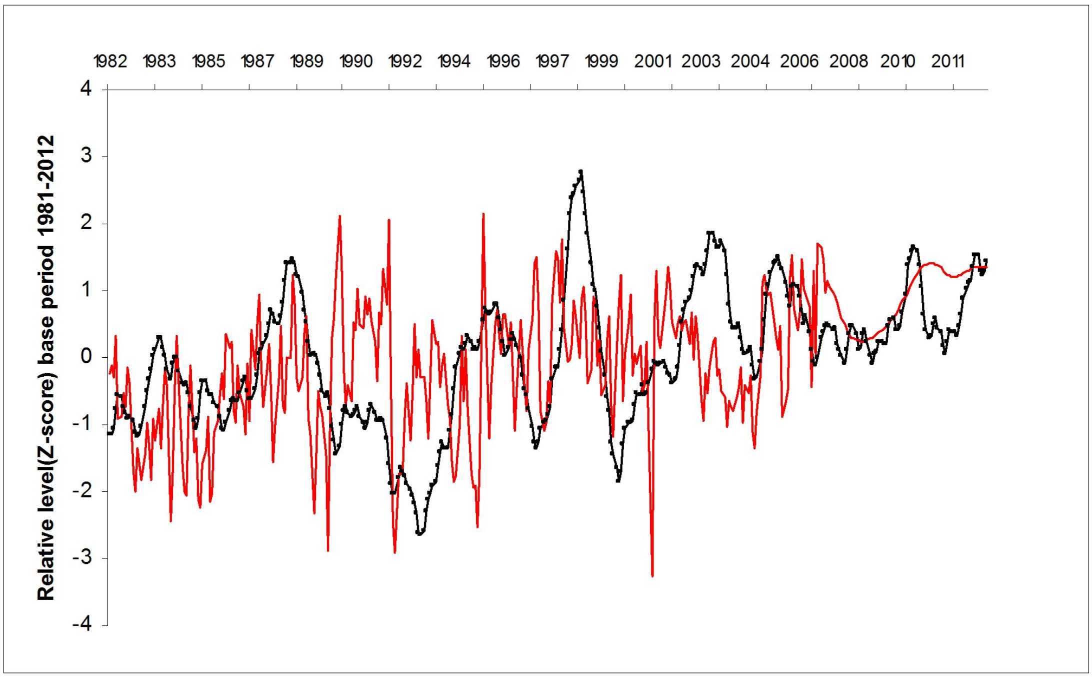

Figure 13. *Z* scored monthly data: NDVI (red curve) compared to first-derivative atmospheric CO_2 smoothed by two 13 month moving averages (black dotted curve).

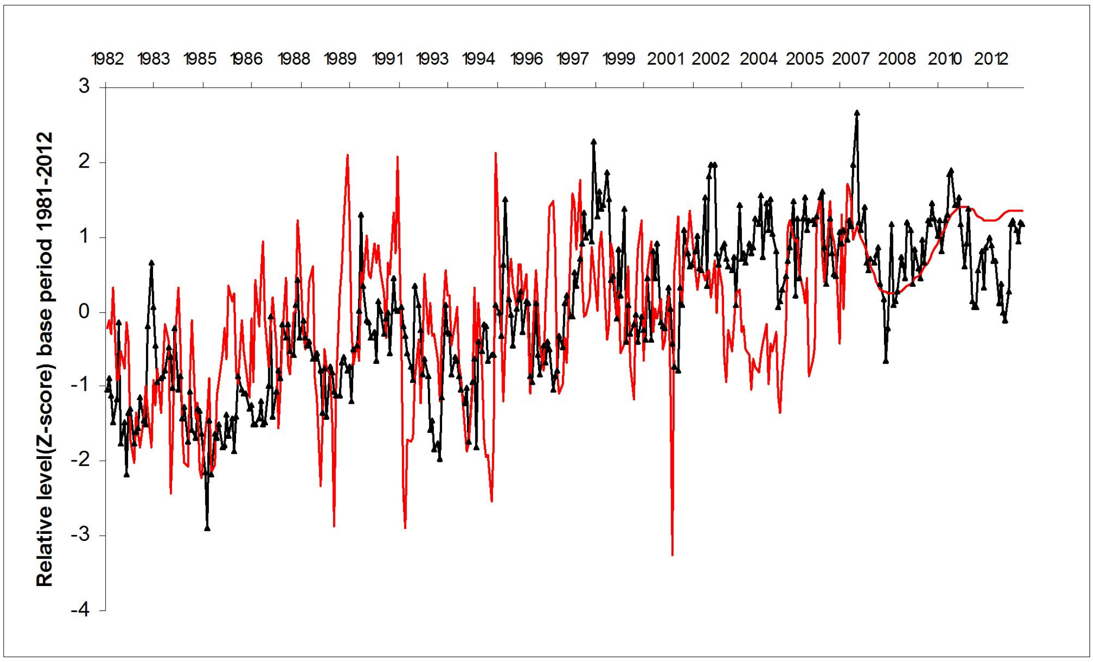

Figure 14. *Z* scored monthly data: NDVI (black curve) compared to the difference between the observed level of atmospheric CO_2 and global surface temperature (red dotted curve).

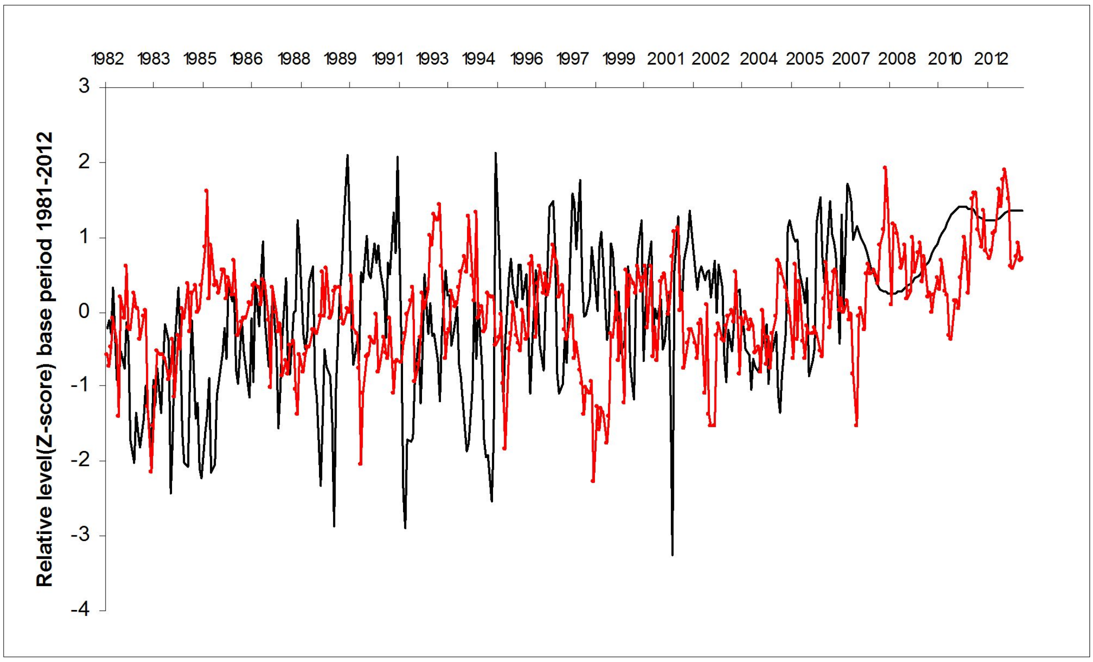

Figure 15. Z scored monthly data: NDVI (black curve) led by 17 months compared to the difference between the observed level of atmospheric CO_2 and global surface temperature (red dotted curve). Months of lead of the NDVI series indicated by OLS dynamic regression modelling

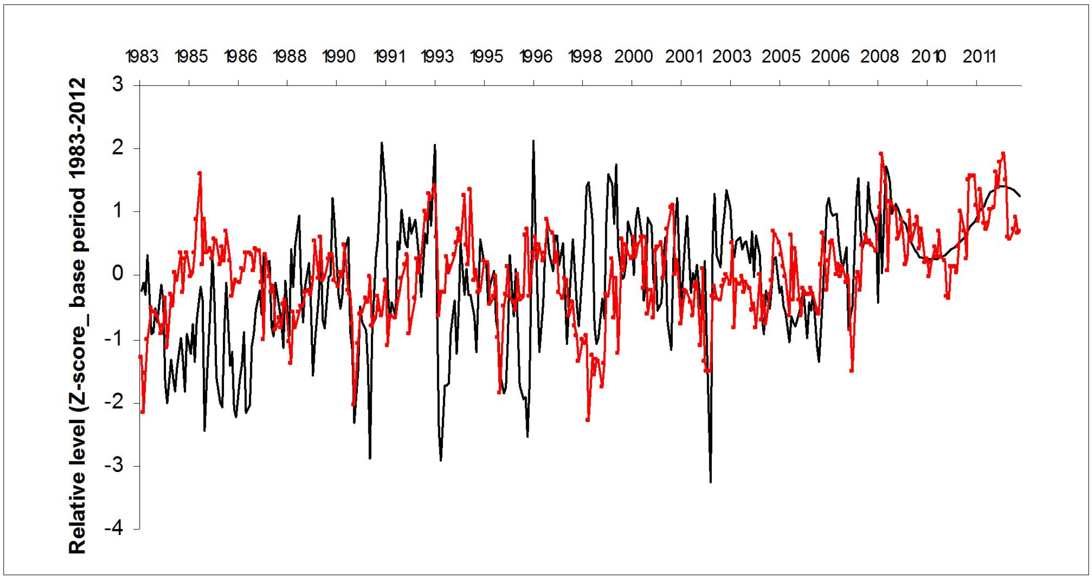

Figure 16. Reverse log probability values (red dotted curve) for lags generated by extensive search of the lag space from lag 2 to lag 40 for the null hypothesis that NDVI does not Granger-cause the difference between the observed level of atmospheric CO_2 and global surface temperature. Green dashed line represents 0.05 level of statistical significance.